Sonochemistry dosimetries in seawater

Rabiaa Khaffache, Aissa Dehane, Slimane Merouani, Oualid Hamdaoui, Hamza Ferkous, Maher M Alrashed, Intissar Gasmi, Atef Chibani

Ultrasonics Sonochemistry 101 (2023) 106647

Contents lists available at ScienceDirect

Ultrasonics Sonochemistry

journal homepage: www.elsevier.com/locate/ultson

Sonochemistry dosimetries in seawater

Rabiaa Khaffache [a], Aissa Dehane [b,*], Slimane Merouani [b], Oualid Hamdaoui [c], Hamza Ferkous [a], Maher M. Alrashed [c], Intissar Gasmi [d], Atef Chibani [e]

[a] Laboratory of Environmental Engineering, Department of Process Engineering, Faculty of Engineering, Badji Mokhtar – Annaba University, P.O. Box 12, 23000 Annaba, Algeria
[b] Laboratory of Environmental Process Engineering, Department of Chemical Engineering, Faculty of Process Engineering, University Constantine 3 Salah Boubnider, P.O. Box 72, 25000 Constantine, Algeria
[c] Chemical Engineering Department, College of Engineering, King Saud University, P.O. Box 800, 11421 Riyadh, Saudi Arabia
[d] Laboratoire Ampère, Ecole Centrale de Lyon, 36 Avenue Guy de Collongue, 69134 Ecully, France
[e] Research Center in Industrial Technologies CRTI, P.O.Box 64, Cheraga 16014, Algiers, Algeria

ARTICLE INFO

Keywords:
Dosimetry
Iodometry
Fricke
4-Nitrophenol
H_2O_2
Ascorbic acid

ABSTRACT

Due to the complex physical and chemical interactions taking place in the sonicated medium, various methods have been proposed in the literature for a better understanding of the sonochemical system. In the present paper, the performance of calorimetry, iodometry, Fricke, 4-nitrophenol, H_2O_2, and ascorbic acid dosimetry techniques have been evaluated over the electric power range from 20 to 80 W (f = 300 kHz). These methods have been analyzed for distilled and seawater in light of the literature findings. It has been found that the lowest temperatures and calorimetric energies were obtained for seawater in comparison to distilled water. However, the discrepancy between both mediums disappears with the increase in the electric power up to 80 W. Compared to the calorimetry results, a similar trend was obtained for the KI dosimetry, where the discrepancy between both solutions (seawater and distilled water) increased with the reduction in the electric power down to 20 W. In contrast, over the whole range of the electric power (20–80 W), the H_2O_2 dosimetry was drastically influenced by the salt composition of seawater, where, I_3^- formation was clearly reduced in comparison to the case of the distilled water. On the other hand, a fluctuated behavior was observed for the Fricke and 4-nitrophenol dosimetry methods, especially at the low electric powers (20 and 40 W). It has been found that dosimetry techniques based on ascorbic acid or potassium iodide are the best means for accurate quantification of the sonochemical activity in the irradiated liquid. As a result, it has been concluded, in terms of the dosimetry process's performance, that the dosimetry methods are in the following order: Ascorbic acid ≈ KI > Fricke > 4-nitrophenol > H_2O_2.

1. Introduction

In recent years, advanced oxidation processes (AOPs) based on the production of hydroxyl radicals (and other powerful oxidants) have proven to be extremely effective methods for the destruction of recalcitrant pollutants [1–4]. Ultrasound (US) is one of the most promising AOPs since it is regarded as a selective method in which toxic and/or resistant hydrophobic chemicals can be destroyed more quickly than those hydrophilic molecules [5,6]. Whereas, due to the relatively low energy efficiency of the sonochemical process, different innovative solutions, such as the use of additives (CCl_4, salts, solid particles, etc.) as well as its hybridization (US/UV, US/O_3, US/Cl, US/H_2O_2, etc.) with other plausible methods, have been proposed for enhancing the sonoefficiency in the irradiated solution [7–10]. On the other hand, it has been found that the modification (composition, concentrations, bubbling of gas, etc.) of the sonicated medium results in a large alteration of its physical and chemical properties (second effect). Therefore, the sonochemical and sonoluminescence behaviour of the bubble population is slightly, not affected, or highly modified [11–14]. As a result, the quantification of the sonochemical and activities in different mediums is of great importance for a better understanding of the sonochemical process.

In literature, several techniques have been developed for a reliable evaluation of the bulk liquid's sonoactivity. These methods include the

* Corresponding author.
E-mail address: aissaleon15@gmail.com (A. Dehane).

https://doi.org/10.1016/j.ultsonch.2023.106647
Received 15 February 2023; Received in revised form 8 October 2023; Accepted 10 October 2023
Available online 21 October 2023

quantification of the generated •OH radicals (e.g. Fricke, Terephthalate, electron spin trapping, iodometry, salicylic acid, H_2O_2, etc.) in addition to sonochemiluminescence, and acoustic mapping methods [15–17]. However, each of these methods has its advantages and disadvantages, which are strongly dependent on the structural composition of the sonoirradiated molecules [17]. For example, Kumar and Chatterjee [18] (20, 23 kHz and 3.5 MHz) found that the evaluation of •OH formation through Fricke dosimetry is more effective for the ferrous sulfate concentration in the range from 1 to 8 mM. On the other hand, in the recent paper of Rajamma et al. (490 kHz) [19], a clear discrepancy was retrieved for the terephthalate dosimetry (8 μM of •OH yield) compared to Weissler (200 μM) and Fricke (289 μM) methods. However, despite the additional products detected during terephthalic acid decomposition, this discrepancy is still unjustified. Therefore, more investigations are needed for a deeper comprehension of the terephthalate dosimetry mechanism. Furthermore, in the experimental work of Merouani et al. (300 kHz) [20], the effects of several operating parameters (reagent's concentration, acoustic power, solution pH, liquid temperature) on Fricke, KI, and H_2O_2 dosimetry techniques have been analyzed. It has been concluded that KI dosimetry was more sensitive to the KI concentration, acoustic energy, and pH, whereas the impact of liquid temperature and acoustic power was more remarkable for Fricke dosimetry. In contrast, the H_2O_2 technique was importantly affected by acoustic power, solution pH and temperature, whereas the efficacy of the three investigated dosimetry approaches (KI, H_2O_2 and Fricke dosimetry) was independent of the solution volume.

Despite the various dosimetry works, until now, no direct investigation has been performed in the presence of seawater. It is of practical interest to evaluate the sonochemical activity in saline waters, since recent reports reflect that salts may play multiple roles depending on substrate physicochemical properties and liquid height [13,21,22]. In the present paper, a detailed investigation was carried out for the analysis of calorimetry, KI, H_2O_2, Fricke, 4-nitrophenol, and ascorbic acid dosimetry methods in seawater and distilled water. This study was conducted at the ultrasound frequency of 300 kHz and over the electric power range from 20 to 80 W. The obtained findings were discussed in light of the different experimental results available in the literature.

2. Experimental protocols

2.1. Reactor

In the present section, the different used sonoreactor characterization techniques are described. It should be noted that all the experimental runs are performed in a standing wave sonoreactor (500 mL volume, as shown in Fig. 1, where the sonicated liquid is irradiated from the bottom, through a Pyrex plate surface (diameter 5 cm) holding the piezoelectric disk (diameter 4 cm), at a frequency of 300 kHz. For all experiments, distilled water or seawater (obtained from The Mediterranean Coast, Annaba city) with a volume of 200 mL is sonicated. The temperature of the cylindrical sonoreactor was adjusted using a water jacket. An electric power (P_E) ranging from 20 to 80 W was delivered to the piezoelectric disk. It should be stressed here that the sonochemical efficiency of the sonicated reactor has been evaluated relying on the different approaches discussed below.

2.2. Procedures

All reagents used in the present work were analytical grade. All runs were performed under an air atmosphere. Sonication was carried out at ambient conditions (25 °C).

- **The calorimetric technique**: For the determination of the effective acoustic power dissipated in the sonicated medium, the initial temperature rise, recorded over 5 min, was measured using a thermocouple, which was held at the half height of the solution (between the transducer and the solution surface) [23], and at a middle distance between the cylinder axis and the internal reactor wall, as shown in Fig. 1. The thermocouple's position was retained over the calorimetric runs. Each measurement was repeated four times to ensure the reproducibility of the results. This procedure was repeated for each electrical power (20, 40, 60, and 80 W). Finally, to minimize heat loss, the reactor jacket was emptied of cooling water. As a result, the acoustic power (P_{ac}, W) transmitted to the medium is determined as follows [20]:

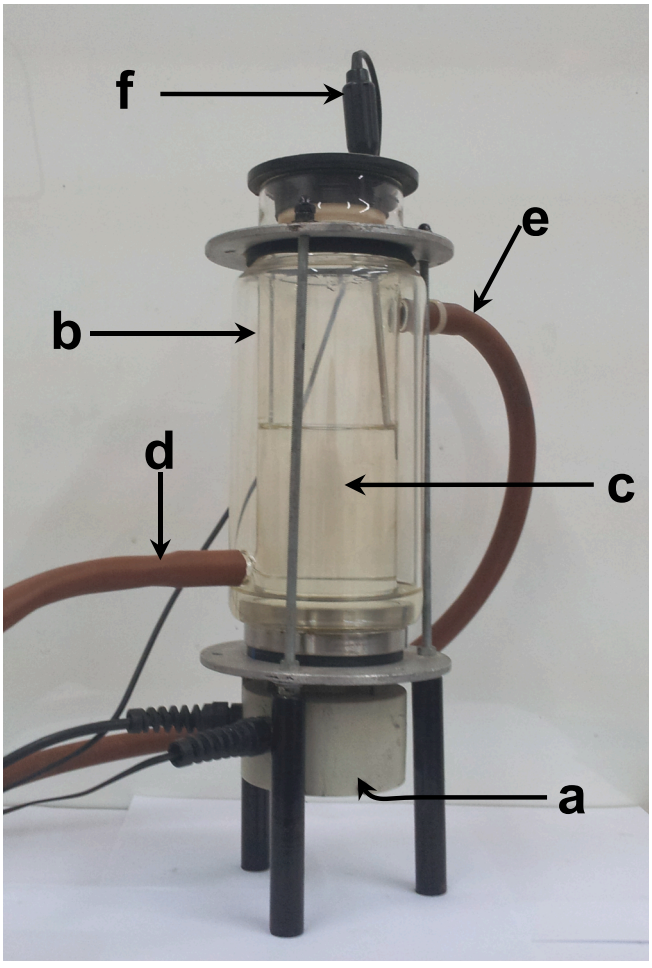

Fig. 1. Picture of sonochemical reactor used for the experimental manipulations. (a) 300 kHz ultrasonic transducer, (b) cylindrical jacketed glass cells, (c) sonicated water, (d) inlet cooling water, (e) outlet cooling water, (f) thermocouple.

$$P_{ac} = mCp\frac{\Delta T}{\Delta t} \quad (1)$$

where, m (g), C_P (4.184 and 3.994 (J g^{-1} K^{-1}) for DW and SW, respectively (at 20 °C) [24,25]) and $\Delta T/\Delta t$ (°C s^{-1}) denote the solution mass, the specific heat at constant pressure and the rate of temperature increase, respectively.

- **Potassium iodide**: Potassium iodide solution (0.1 M) was irradiated in the above-described sonoreactor. The absorbance of I_3^- at the maximum wavelength of 352 nm (ε = 26,000 L mol^{-1} cm^{-1}) was recorded with a UV–Vis spectrophotometer (Jenway 6405). The spectrophotometric (at 352 nm, ε = 26,000 L mol^{-1} cm^{-1}) monitoring of I_3^- ions allows us to quantify the amount of •OH radicals as a function of the sonication time [20,26]. Due to the linearity of the formation of I_3^- versus time, the different measurements (using KI

dosimetry) were compared based on the formation rate of I_3^- obtained after 30 min of sonication.

- **Fricke dosimetry:** In an acidic medium, the ultrasonic irradiation of a Fricke solution causes Fe^{2+} ions to be oxidized to Fe^{3+} ions. The absorbance of Fe^{3+} at 304 nm was measured by UV spectrophotometer ($\varepsilon = 2197$ L mol^{-1} cm^{-1}). The Fricke solution was prepared with $FeSO_4(NH_4)_2$ $SO_4{\cdot}6H_2O$ (10^{-3} M), H_2SO_4 (0.4 M) and NaCl (10^{-3} M) [19,20].
- **Hydrogen peroxide (H_2O_2) production**: The concentrations of hydrogen peroxide (H_2O_2) were determined using the iodometric method [27,28]. If there are not any solutes in the bulk solution, the primary radicals recombine at the bubble–solution interface to form hydrogen peroxide (H_2O_2) according to the following reactions [29,30]:

$$2^{\cdot}OH \rightarrow H_2O_2 \quad k_1 = 5.5 \times 10^9 M^{-1}s^{-1} \tag{2}$$

$$2HO_2^{\cdot} \rightarrow H_2O_2 + O_2 \quad k_2 = 8.3 \times 10^5 M^{-1}s^{-1} \tag{3}$$

As $k_1 \gg k_2$, the production of H_2O_2 can be used to estimate the amount of OH radicals generated by acoustic cavities. Therefore, in the presence of excess iodide ions, the reaction between I^- and H_2O_2 was catalyzed via heptamolybdate. The formed triiodide ion, (I_3^-), was monitored at a wavelength of 352 nm ($\varepsilon = 26{,}000$ L mol^{-1} cm^{-1}). In the quartz cell of the spectrophotometer containing potassium iodide (1 mL, 0.1 M) and ammonium heptamolybdate (20 μL, 0.01 M), sample aliquots (200 μL) collected from the reactor were added. Before measuring the absorbance, the combined solutions were allowed to stand for 5 min.

- **4-Nitrocatechol (4-NC) dosimetry**: The concentration of 4-Nitrocatechol (4-NC), resulting from the oxidation of 4-nitrophenol (10^{-3} M) under the action of hydroxyl radicals [31], was measured spectrophotometrically in 0.1 M NaOH at 512 nm (ε = 12,500 M^{-1} cm^{-1}).
- **Ascorbic acid dosimetry**: The temporal evolution of ascorbic acid concentration ($C_0 = 10^{-4}$ M) was followed using a UV spectrophotometer at the wavelength of 260 nm [32,33].

It should be noted that for each of the above-described monitoring techniques, a sample of 1 mL has been withdrawn from the sonicated solution (with the exception of H_2O_2 production method) to quantify the monitoring species.

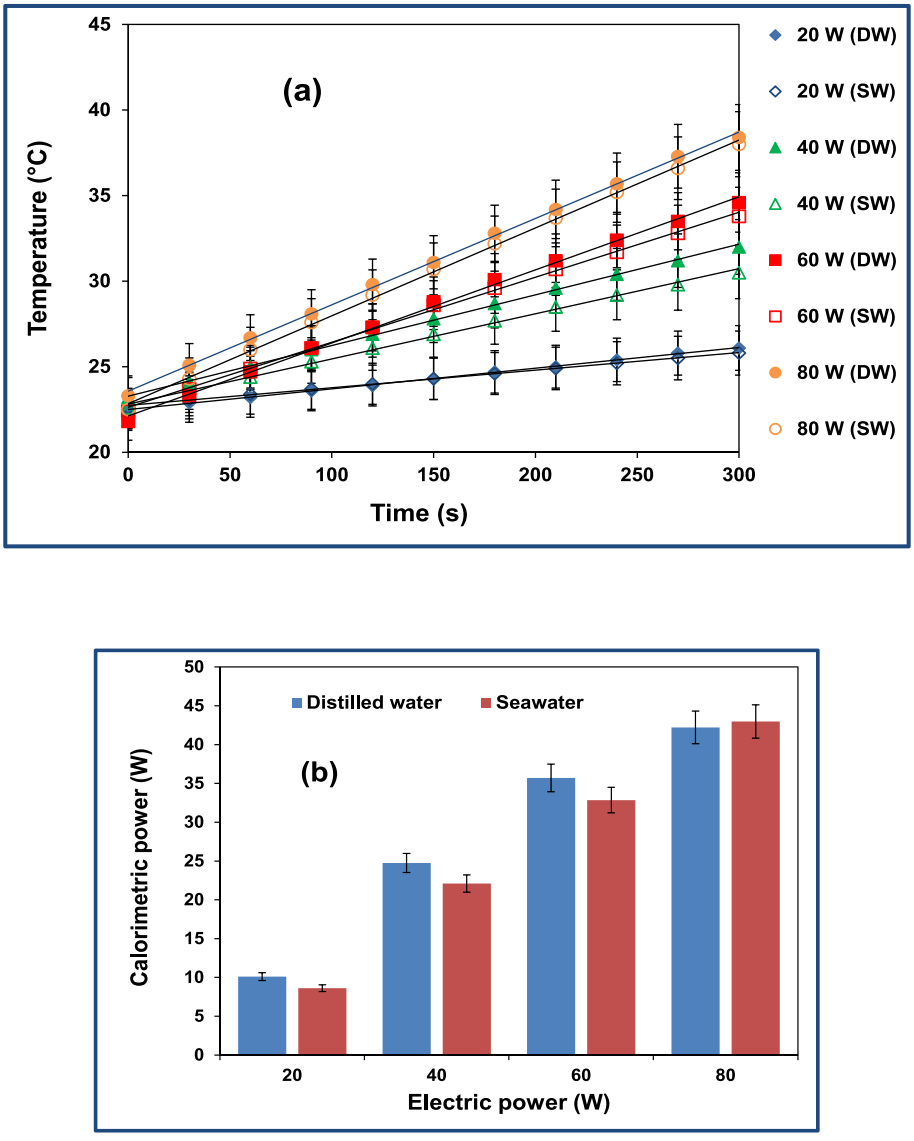

Fig. 2. Temporal evolution of bulk temperature (a) and calorimetric power dissipated in seawater "SW" and distilled water "DW" (b) as a function of electric power (from 20 to 80 W) at 300 kHz. (for (a): $R^2 > 0.99$).

3. Results and discussions

3.1. Calorimetry

In Fig. 2(a) and (b), the evolution of bulk temperature and calorimetric energies are shown for both mediums (i.e., distilled water and seawater) under the same operating conditions (duration = 300 s, f = 300 kHz, P_E = 20–80 W). From Fig. 2 (a) it can be seen that over a phase of 300 s, the temperature increase (ΔT) in distilled water is 2.16, 2.97, and 7.83 % greater than that in seawater for the electric powers of 20, 40, and 60 W, respectively, whereas, at the electric power of 80 W, the increase in seawater temperature is 4.08 % greater than that in distilled water. The same trend was retrieved for the calorimetric energy (ultrasonic or acoustic energy) dissipated in the sonicated medium [Fig. 2 (b)]; however, for both cases, the acoustic energy is ~50 % of the electrical power, which is in line with many literature findings [17,34,35]. At 20, 40 and 60 W, the calorimetric power in distilled water is 17.42, 11.99, and 8.68 % greater than that in seawater. In contrast, at 80 W, the measured calorimetric energy in seawater is 1.8 % greater than that in distilled water, as shown in Fig. 2(b). According to Fig. 2(a) and (b), it seems that for the electrical power in the range from 20 to 60 W, the distilled water is dominant (compared to seawater) in terms of liquid temperature and calorimetric increases (at 80 W, the seawater is dominant). A direct explanation of the observed trends in Fig. 2(a) and (b) is not possible due to the multiple interferences between the impacts of different physical parameters (e.g., viscosity, vapor pressure, surface tension) affecting the energetic behavior of our mediums (seawater and distilled water).

However, some elucidations are possibly given to explain the obtained results in Fig. 2(a), (b). It is noteworthy to indicate that according to Tuziuti et al. [36], the increase in liquid temperature in principally due to the heat conducted outside the collapsing bubbles toward the bulk liquid in addition to the friction between the liquid and the oscillating bubbles (viscous interactions). In contrast, according to Son et al. [17,37], the contribution of the cavitational energy to heat generation (and temperature increase) is lower (<14 %) than that caused by sound absorption. Furthermore, an energetic classification (dissipation, atomization, transducer heating and heat loss toward surroundings) has been proposed for the electric energy input [38,39]. As it can be retrieved from the previous studies [17,36,37], an exact quantification of the contribution of each energy source and transformation is a difficult task, especially with the variation of the experimental conditions (liquid height, viscosity, ultrasound frequency, acoustic amplitude, etc.).

On the other side, it is known that due to the transmission of an ultrasonic wave into a liquid, the molecules of this medium vibrate under the action of the sound wave. Therefore, viscous interactions take place between these molecules, which convert the acoustic energy [mechanical (kinetic) energy] into heat; consequently, the absorption of this degraded acoustic energy by the sonicated medium gives rise to the small increase in liquid temperature thanks to the application of high acoustic power. In general, in a liquid, the attenuation/absorption coefficient (α) as a function of viscosity and thermal conduction is given by [17,40–42]:

$$\alpha = \frac{2\pi^2 f^2}{\rho c^3}\left[\frac{4}{3}\eta_s + \frac{(\gamma-1)\kappa}{C_p}\right] \quad (4)$$

where η_s is the ordinary (or shear) viscosity of the liquid, f is the applied frequency, ρ is the density of the liquid, c is the sound velocity in the liquid, γ is the specific heat ratio, κ is the thermal conductivity, and C_p is the heat capacity at constant pressure.

However, as it is given in [40,41], the same attenuation coefficient (6.33×10^{-5} dB/cm at 20 °C) is obtained for both cases (seawater and distilled water); therefore, the observed discrepancy in Fig. 2(a), (b) are preferably analyzed through the effect of the cavitational energy (rather than sound absorption). It is known that for a single bubble, a small amount of energy is evacuated outside the acoustic cavitation (from the hot spot) towards the surrounding liquid. Nevertheless, for millions of bubbles, this cavitational energy may partly contribute to the rise in liquid temperature when an intense sonication is transmitted in the liquid [43–45]. On the other hand, it is well established that the presence of salt in water leads to the reduction of gas solubility (salting out effect); therefore, smaller bubbles (with high sonochemical and sonoluminescence activity) are formed, which reduces the extent of bubble coalescence and clustering as well as the attenuation of the ultrasonic irradiation [46–50]. This is the case in the present study ([NaCl] ≈ 0.6 M) as the sonoactivity of bubbles (strong collapses) is expected to be increased in accordance with the different experimental works [7,51]. However, with the reduction of bubble volume, less heat energy is dissipated outside the collapsing bubbles, which means that the increase in liquid temperature is lower in seawater compared to the case of distilled water.

On the other hand, as can be seen in Table 1, except for viscosity, the presence of salts seems to have a slight impact on the physical properties of water. In the presence of salty water ([NaCl] ≈ 35 g/L) a variation of +2.6, −0.94, +7.75, +1.38, and +2.67 % is registered for density, vapor pressure, dynamic viscosity, surface tension, and sound speed, respectively, in comparison to distilled water. As a result, the probable effects of vapor pressure and surface tension are excluded. This is despite the fact that smaller bubbles (Laplace pressure (2σ/R) goes up) are formed in seawater [46,47]. It is worth mentioning that the effect of surface tension is only important during the nucleation phase. Therefore, more stabilization of bubbles is observed after the nucleation process, and more cavities are expected to grow to active size without breaking apart [52,53]. On the other hand, the viscosity parameter (7.75 % of increase in seawater) may have a relatively important effect on the dynamics of bubbles in the sonicated seawater. Therefore, bubble oscillation is dampened in seawater compared to that in distilled water. Consequently, collapse intensity as well as the heat evacuation outside the bubble goes down. Shen et al. [54] (f = 26.5 kHz, P_A = 1.325 atm) have demonstrated that the maximum bubble temperature and pressure are reduced proportionally with the increase in total viscosity with/or without accounting for bulk viscosity (important only at high acoustic amplitudes and high viscosities [54–56]). Furthermore, it should be noted that the impact of the liquid viscosity at the bubble wall is reduced at the end of the collapse phase, due to the increase in the interfacial temperature of cavitation [57].

In light of the above discussion, it can be deduced that the lower temperature and calorimetric energy obtained in seawater compared to the distilled water are mainly ascribed to the lower heat evacuated outside of the small bubbles (low surface) formed in seawater and the decrease in bubble collapse intensity with the rise in seawater viscosity. However, with the increase in the electric power to 80 W, it has been observed that the impact of these controlling parameters (small exchange surface of bubbles and the relatively high viscosity in seawater) vanishes. As a result, this led to a 4.08% and a 1.8 % of increase, respectively, in the liquid temperature and calorimetric energy in seawater, as shown in Fig. 2(a) and (b). This trend is attributed to the fact that at 80 W, more bubble expansion (higher expansion ratio, R_{max}/R_0) is expected to take place in seawater, with the reduction of the

Table 1
Physical properties of salty and distilled waters at 25 °C [104].

Sample	Density [kg/m^3]	Vapor pressure [kPa]	Dynamic viscosity [Pa.s]	Surface tension [N/m^2]	Speed of sound [m/s]
Distilled water	997	3.170	0.890×10^{-3}	0.072	1494
35 (g/L) NaCl solution	1023	3.140	0.959×10^{-3}	0.073	1534

damping effect of viscosity. Therefore, stronger collapses of bubbles and higher contact surfaces are obtained (at 80 W), which leads to more heat evacuation toward the surrounding salty water. In contrast, for distilled water (already containing a larger number of nucleus), the increase in energy input to 80 W increases the extent of bubble coalescence (compared to seawater), which leads to the formation of relatively larger bubbles in which the overall collapse intensity is reduced (milder collapses). This means that the rise of the energy input to 80 W has a negative impact on the energetic behavior of the distilled water in terms of temperature increase and the dissipated calorimetric energy.

3.2. KI dosimetry

Under the electric power ranging from 20 to 80 W (Fig. 3 (a)), the temporal evolutions of I_3^- concentration are shown over a duration of 30 min for both mediums. In Fig. 3 (b), the formation rates of I_3^- (over 30 min) are given at 20, 40, 60 and 80 W. As can be seen in Fig. 3 (a), as a function of time, the molar yield of I_3^- is proportionally increased with the rise in electric power (from 20 to 80 W) either in seawater or in distilled water, following a zero-order kinetic law. Whereas, according to Fig. 3 (b), it can be retrieved that the difference in I_3^- production rate ($\mu M\ min^{-1}$), between distilled water and seawater, is energy input dependent. Compared to the distilled water, the production rate of I_3^- in seawater is decreased by 6.45 and 6.77 %, respectively at 20 and 40 W. This difference goes down to 1.71 and 1.66 % at 60 and 80 W, respectively, as shown in Fig. 3 (b).

It is noteworthy to indicate that a great discrepancy is observed in the literature for the sonochemical yield of I_3^- in the presence of different salts. For example, Gogate and Katekhaye [58,59] retrieved an increase of ~2 times in I_3^- production through the sonication (20 and 204 kHz) of air-saturated water in the presence of NaCl (0.034–0.34 M) and $NaNO_2$ (0.029–0.29 M). Tuziuti et al. [48] have demonstrated the existence of an optimum air concentration (4.2 mg/L) for the maximal I_3^- absorption and scattered light intensity (an indicator of active bubble number). According to Wood et al. [34], the enhancement (increase and expansion of SL active regions) of sonoluminescence [at 44 kHz ([KI] from 0.1 to 1 M) and 300 and 1000 kHz ([KI] from 0.1 to 2 M)] was ascribed to the decrease in gas concentration (due to the presence of I^-) and its multiple benefits such as the reduction of wave attenuation, bubble clustering, and coalescence. This positive impact was increased with the rise in ultrasonic power (depending on the applied frequency) as well as the application of flow, surface stabilization at high salt (KI) concentrations. On the contrary, the decrease in sonoluminescence intensity at higher KI concentrations (>1 M at 44 kHz and > 2 M at 300 and 1000 kHz) was linked to the reduction in the energy of collapse (of smaller bubbles). On the other side, Gutérrez et al. [60] have found (at 1 MHz) that the production rate of I_3^- is constant for $MgCl_2$ concentration up to 0.1 M in CCl_4-saturated solution (2 M in the absence of CCl_4). Above these concentrations (i.e., 0.1 and 2 M), the yield of I_3^- was drastically decreased. This trend (decrease in I_3^- formation) was correlated to the

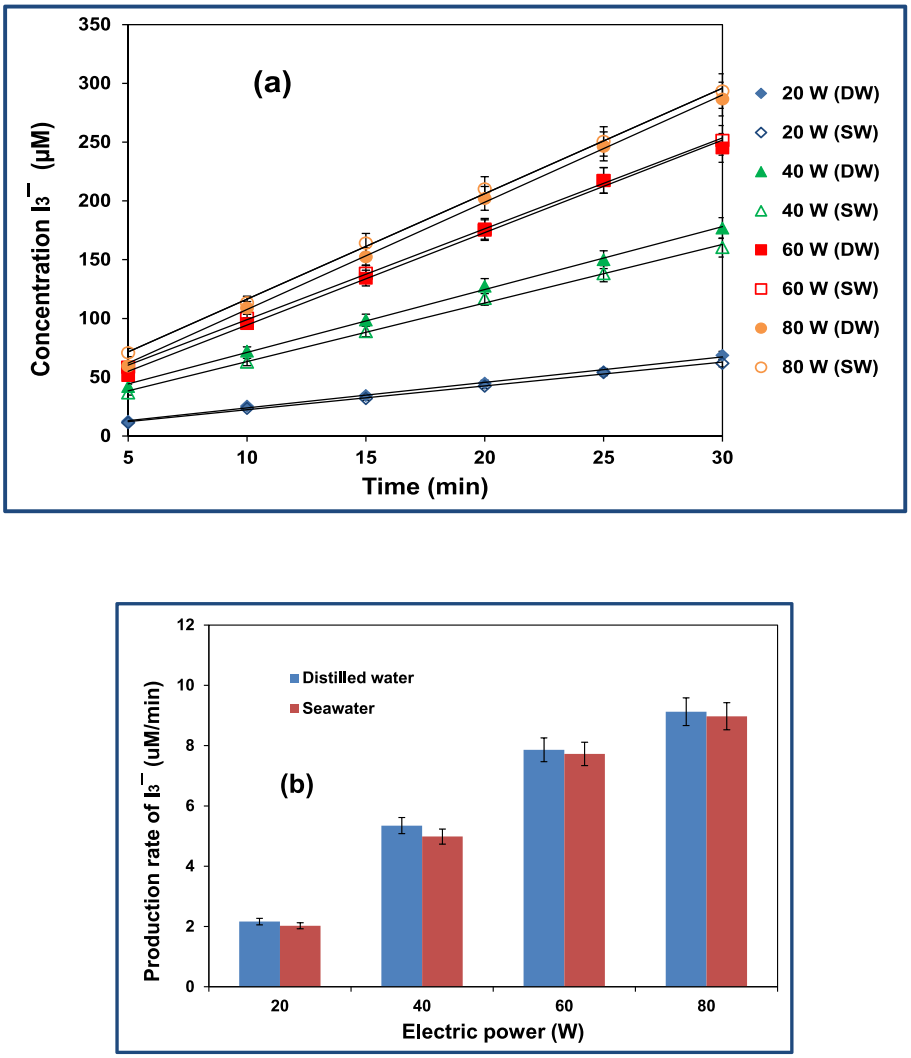

Fig. 3. Temporal variation of triiodide concentration (a) and its production rate (b) for the same conditions as in Fig. 2. (for (a): $R^2 > 0.99$).

increased liquid viscosity (reduces the collapse intensity of bubbles). Similarly, Lepoint et al. [61] (1.6 MHz) reported a sharp decrease in I_3^- formation for $MgCl_2$ concentration between 2×10^{-3} and 3×10^{-3} M. This was explained by a change in the electrokinetic potential of the bubbles.

In light of the above results, a clear discrepancy is observed between the different works regarding the impact of salts on the sonochemical activity (explained in terms of I_3^- formation) in the sonicated solution. According to Fig. 3(a) and (b), it seems that the effect of seawater is relatively accentuated at 20 and 40 W, while this effect relatively goes down at 60 and 80 W. This behavior could be explained by the dampness of bubble dynamics at 20 and 40 W thanks to the relatively increased viscosity (see the previous section); therefore (at 20 and 40 W) the collapse intensity of bubbles is reduced, which is translated by low I_3^- formation. Consequently, a decrease of 6.45% and 6.77 % in I_3^- production rate is obtained at 20 and 40 W, respectively. On the other hand, at 60 and 80 W, the negative effect of seawater is exceeded giving approximately the same yielding rate of I_3^- as in the distilled water.

On the other hand, considering the effect of salts on the gas concentration and the behavior of different species present in the bulk solution, it can be indicated that due to the existence of salts (Table 2) in the irradiated solution, a "salting-out effect" is exerted on both, the gas concentration and iodide distribution in the irradiated solution. Because iodide is a nonvolatile, hydrophilic substance with high solubility (144.5 W% at 20 °C [62]), this element is principally found in the bulk solution. Thus, in seawater, the ionic strength of the solution is increased, which means that iodide is pushed (fewer water molecules are available to dissolve iodide) toward the bubble/liquid interface where hydroxyl radicals are likely to occur quickly [11,63]. This mechanism (salting-out effect) has been indicated in several experimental works showing the improvement of the sono-degradation of pollutants [11,14,63,64] in the presence of various salts (such as NaCl, $NaNO_3$, $NaNO_2$ and Na_2SO_4). Gogate et al. [58] have marginalized the salting-out effect on iodide in the presence of NaCl (0.2 % w/w). However, in this study, a very low concentration of I^- (0.0018 M) was used compared to the present work (0.1 M). On the other hand, according to Brotchie et al. [46], the impact of salts was completely ascribed to the salting-out effect on the dissolved gas (not on the substrate molecules), where the rise in salt dose causes the concentration of gases to be decreased. As a result, the bubbles' coalescence, clustering and irradiation attenuation go down, which resulted in smaller bubbles of high sonochemical and sonoluminescence activity. This conclusion is supported by the findings of Wall et al. [7], where the increase in sonoluminescence intensity was well correlated to the decrease in the dissolved gas concentration (rather than solution viscosity, vapor pressure, surface tension, or ionic strength) and the increase in salt dose. In contrast, Uddin et al. [65] have considered the decrease in gas solubility (depending on the salt nature) as a negative effect of salts (Na_2SO_4 and NaCl) on the sonoactivity of the solution, thanks to the decreased number of bubbles.

Table 2
Main characteristics of seawater [67,105–107].

	Seawater
pH	7.6
Ca^{2+}	0.4 g/L
Mg^{2+}	1.3 g/L
Na^+	11.0 g/L
K^+	–
Cl^-	20.0 g/L
SO_4^{2-}	3.0 g/L
HCO_3^-	–
Br^-	0.065–0.08 g/L
TOC[a]	~ 1.2–1.5
COD[b]	0.00271–0.00469 g/L
BOD_5[c]	0.00178–0.00292 g/L
TDS[d]	10–100 g/L
λ[e]	0.598 Wm^{-1} K^{-1}

[a] Total organic carbon.
[b] Chemical oxygen demand.
[c] BOD_5: biological oxygen demand.
[d] Total dissolved solids.
[e] Thermal conductivity (at 20 °C).

In addition to the effects of salting-out process and viscosity, it is known that Cl^- and Br^- are good free radicals (such as •OH, Cl•) scavengers [Reactions (5)-(15), respectively] [66,67] (compete with I^- for the reaction with •OH), this inhibiting effect is increased especially at high concentrations of Cl^- (20 g/L, Table 2) and Br^- (65–80 mg/L, Table 2), where this process is shifted toward bubble/liquid interface. However, the resulting chlorine and bromide radicals (less efficient than •OH, Reactions (5)–(15)) are expected to be contributors to the oxidation of iodide. Thus, the production rate of I_3^- in seawater is found to be close to that generated in distilled water.

$$Cl^- + {}^{\cdot}OH \rightarrow ClOH^{\cdot -} \quad k_5 = 4.3 \times 10^9 M^{-1}s^{-1} \tag{5}$$

$$FeCl^+ + HO_2^{\cdot} \rightarrow HO_2^- + Fe^{3+} + Cl^- \quad k_{30} = 1.2 \times 10^6 M^{-1}s^{-1} \tag{6}$$

$$Cl^{\cdot} + Cl^- \leftrightarrow Cl_2^{\cdot -} \quad k_7 = (5.6 - 12) \times 10^9 M^{-1}s^{-1}, k_{-7} = (6 - 11) \times 10^4 M^{-1}s^{-1} \tag{7}$$

$$Br^- + {}^{\cdot}OH \leftrightarrow BrOH^{\cdot -} \quad k_8 = 1.1 \times 10^{10} M^{-1}s^{-1}, \; k_{-8} = 3.3 \times 10^7 M^{-1}s^{-1} \tag{8}$$

$$BrOH^{\cdot -} \rightarrow Br^{\cdot} + OH^- \quad k_9 = 1.9 \times 10^8 M^{-1}s^{-1} \tag{9}$$

$$BrOH^{\cdot -} + Br^- \rightarrow Br_2^{\cdot -} + OH^- \quad k_{10} = 1.9 \times 10^8 M^{-1}s^{-1} \tag{10}$$

$$Br^{\cdot} + Br^- \leftrightarrow Br_2^{\bullet -} \quad k_{11} = 1.2 \times 10^{10} M^{-1}s^{-1}, k_{-11} = 10^5 M^{-1}s^{-1} \tag{11}$$

$$Cl^{\cdot} + Br^- \leftrightarrow ClBr^{\cdot -} \quad k_{12} = 1.2 \times 10^{10} M^{-1}s^{-1}, k_{-12} = 1.9 \times 10^3 s^{-1} \tag{12}$$

$$Cl_2^{\cdot -} + Br^- \leftrightarrow ClBr^{\cdot -} + Cl^- \quad k_{13} = 4.0 \times 10^9 M^{-1}s^{-1}, k_{-13} = 1.1 \times 10^2 s^{-1} \tag{13}$$

$$Br_2^{\cdot -} + Cl_2^{\cdot -} \rightarrow Br_2 + 2Cl^- \quad k_{14} = 4.0 \times 10^9 M^{-1}s^{-1} \tag{14}$$

$$ClOH^{\cdot -} + Br^- \leftrightarrow ClBr^{\cdot -} + OH^- \quad k_{15} = 1.1 \times 10^9 M^{-1}s^{-1}, k_{-15} = 3 \times 10^6 s^{-1} \tag{15}$$

A limited enhancement (up to 1 mM) was observed for the degradation of RG12 in the presence of Cl^- and Br^- in the UV/chlorine system [67], whereas, even with the raise of these ions' dose up to 50 mM, no inhibiting effect was registered for the RG12 decay. The positive impact of Cl^- was ascribed to the $Cl_2^{\bullet -}$ (2.13 V *vs* NHE) formation (Reaction (5)-(7)) [67–69]. However, its recombination and inhibiting reactions towards •OH, Cl•, Br^-, and $Br_2^{\bullet -}$ (Reactions (13), (14), and (16)-(18)) play a negative role for the oxidizing capacity in seawater:

$$Cl_2^{\cdot -} + Cl_2^{\cdot -} \rightarrow Cl_2 + 2Cl^- \quad k_{16} = 6.3 \times 10^8 M^{-1}s^{-1} \tag{16}$$

$$Cl_2^{\cdot -} + {}^{\cdot}OH \rightarrow HClO + Cl^- \quad k_{17} = 1 \times 10^9 M^{-1}s^{-1} \tag{17}$$

$$Cl_2^{\cdot -} + {}^{\cdot}Cl \rightarrow Cl_2 + Cl^- \quad k_{18} = 2.1 \times 10^9 M^{-1}s^{-1} \tag{18}$$

Similarly, the positive impact of Br^- is possibly reversed by the inhibiting radicals' recombination (Reactions (8), (11)-(13), (15), and (19)-(22)) [67,70,71]:

$$Br_2^{\cdot -} + Cl_2^{\cdot -} \rightarrow Br_2 + 2Cl^- \quad k_{19} = 4 \times 10^9 M^{-1}s^{-1} \tag{19}$$

$$Br_2^{\cdot -} + {}^{\cdot}OH \rightarrow HOBr + Br^- \quad k_{20} = 1 \times 10^9 M^{-1}s^{-1} \tag{20}$$

$$BrCl^{\cdot -} + {}^{\cdot}OH \rightarrow BrCl + OH^- \quad k_{21} = 1 \times 10^9 M^{-1}s^{-1} \tag{21}$$

$$Br_2^{\cdot-} + Br_2^{\cdot-} \rightarrow Br_2 + 2Br^- \quad k_{22} = 1.9 \times 10^9 M^{-1}s^{-1} \tag{22}$$

In general, the enhancing effect of the different ionic species is very dependent on their concentration and reactivity, and the physical properties, concentration of the target substances as well as their reactivity with the generated active species [4,64,67].

In addition to the salting-out effect, viscosity and the impacts of different anions (Cl^- and Br^-), Pflieger et al. [51] indicated that the Cl• atom resulting from the homolytic cleavage of NaCl (inside the bubble), may also contribute to the oxidation of iodide, which enhances the production rate of I_3^-. This effect is probably enhanced by the increase in acoustic power. However, through the experimental study of Pflieger's team [51], the generated Cl• and Na• may also lead to the reduction of the sonoactivity of bubbles (especially H_2 and H_2O_2 formation) via their reactions with •OH and H atoms. On the other hand, it should be noted that no effect is expected in the presence of sulfate ions (3 g/L, Table 2) on the oxidation of iodide thanks to the inertness of SO_4^{2-} toward •OH-based AOPs [4,67,72–74].

In light of the foregoing, it can be deduced that the performance of KI dosimetry in seawater is the result of the competition between the affecting parameters (salting-out effect, viscosity and anions) that influence the oxidation of iodide within the sonicated seawater. As a result, approximately the same performance of KI dosimetry is obtained in seawater and distilled water with an increase in electric power to 60 and 80 W. In contrast, some discrepancy between both mediums is observed at lower electric power, i.e., 20 and 40 W (Fig. 3(a), (b)). Therefore, KI dosimetry could be adopted with confidence for a reliable determination of the sono-irradiated medium.

3.3. H_2O_2 production

Contrary to the obtained results for KI dosimetry (previous section), the findings of Fig. 4(a) and (b) indicate that the yield of H_2O_2 is substantially affected in the case of seawater. This is evidenced in Fig. 4(a), where, the concentrations of H_2O_2 in seawater are clearly lowered compared to those retrieved in distilled water. The outcomes of Fig. 4(a) are translated in Fig. 4(b) as the lowest production rates of hydrogen peroxide are observed in the seawater medium. For example, at 20 W, the formation rate of H_2O_2 is 1.82 and 0.46 μM min^{-1}, respectively, in distilled and seawater. The rise of electric power to 80 W increases these production rates to 8.24 (distilled water) and 3.99 (seawater) μM min^{-1}. Obviously, the variation of the dosimetry technique affects its interactions with the different species present in the irradiated solution. A great part of the statements indicated in the previous section could be adopted to explain the findings of Fig. 4(a) and (b). However, compared to the case of KI dosimetry [Fig. 3(a), (b)], the effect of the different scavenging species toward H_2O_2 (resulting from •OH recombination at the bubble/liquid interface) production seems to be more pronounced. This may be explained by the additional amortization of H_2O_2 formation (in addition to the scavenging of •OH and Cl•, Reactions (5), (7), (8) and (12)) with the scavenging action of the reactive chlorine species

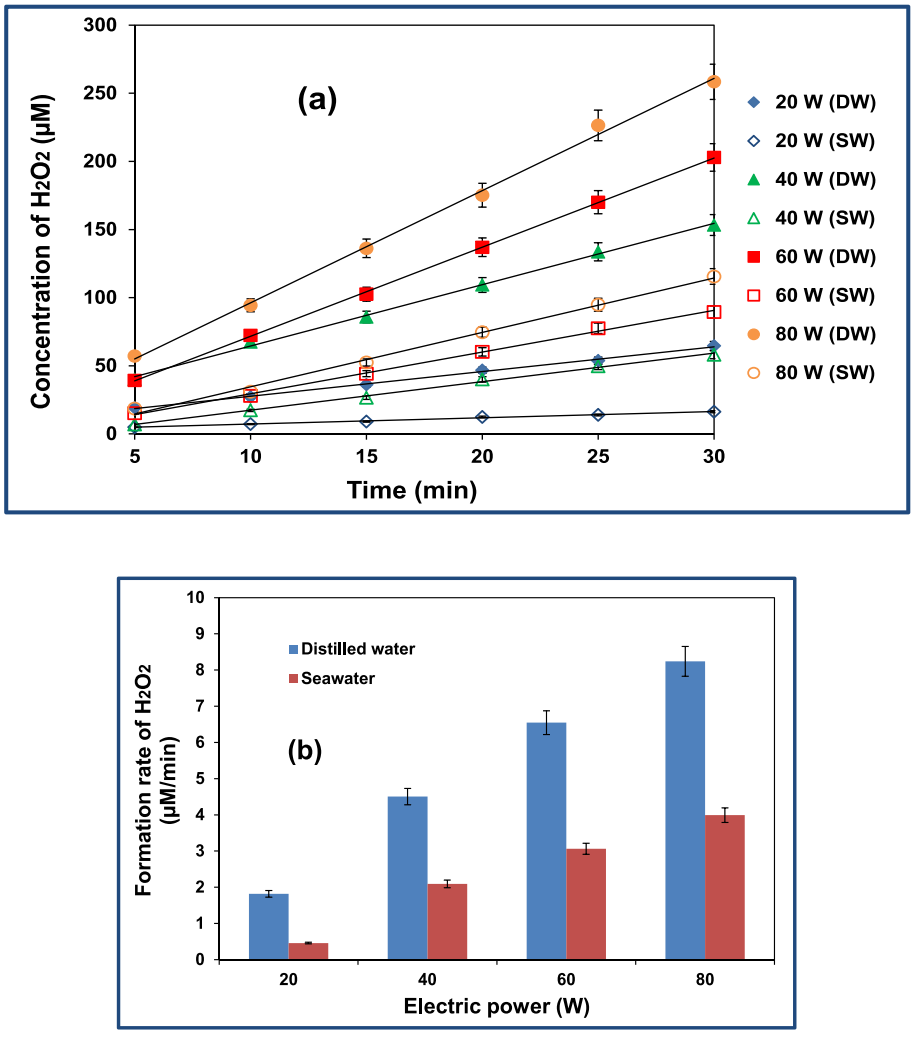

Fig. 4. Temporal evolution of hydrogen peroxide concentration (a) and its production rate (b) for the same conditions as in Fig. 2. (for (a): $R^2 > 0.99$).

[Reactions (23)-(25)] resulting from reactions (5)-(7) as well as the hemolytic dissociation of NaCl inside the bubble [51,75]:

$$Cl^{\cdot} + H_2O_2 \rightarrow HO_2^{\cdot} + Cl^- + H^+ \quad k_{23} = 1 \times 10^9 M^{-1}s^{-1} \tag{23}$$

$$Cl_2^{\cdot -} + H_2O_2 \rightarrow HO_2^{\cdot} + 2Cl^- + H^+ \quad k_{24} = 1.4 \times 10^5 M^{-1}s^{-1} \tag{24}$$

$$Cl_2^{\cdot -} + HO_2^{\cdot} \rightarrow 2Cl^- + H^+ + O_2 \quad k_{25} = 3.1 \times 10^9 M^{-1}s^{-1} \tag{25}$$

According to the experimental findings of Pflieger et al. [51], the reduced production of H_2 and H_2O_2 (with the increase in NaCl concentration up to 5 M) was ascribed to the scavenging process of •OH and •H atoms by Cl• and Na•. Nevertheless, with the consideration of the above chemical reactions [Eqs. (23)-(25)], it is clearly evidenced that the inhibiting chemistry on H_2O_2 formation at the bubble interface should be taken into account. Moreover, Wakeford et al. [76] (35 kHz) have ascribed the decrease in H_2O_2 production to the scavenging of hydroxyl radicals by Cl^- ([NaCl] increased up to 20 %, w/v), whereas the variation of dissolved gas concentration was not considered in this study. In contrast, Uddin et al. [65] have indicated that the decrease in the H_2O_2 yielding was mainly explained by the low dose of dissolved argon gas in the presence of Na_2SO_4 (1–1.5 M) or NaCl (0–1.4 M), where the lowering effect of Na_2SO_4 (with lower solubility of Ar) was greater than that of NaCl. The results of Uddin's group are supported by Okitsu et al.'s findings [77] for which the yield of H_2O_2 (cavitation sonoactivity) was proportionally increased with the amount of dissolved gases (He, Ne, Ar, Kr and Xe). In contrast, Brotchie et al. [46] have shown that the production of H_2O_2 is proportionally increased with the increase in salts' ($NaClO_4$, $NaNO_3$) concentration (and reduction in dissolved gas amount). These outcomes were ascribed to the reduction in bubble coalescence, irradiation attenuation and the increase in bubbles collapse intensity with the increase in salts concentration.

To recap, with the consideration of all the discussed results in the present section, it can be indicated that the overall effect of seawater on H_2O_2 dosimetry is negative, independently of the applied electric power (20–80 W), as shown in Fig. 4(a), (b). This indicates the sensitivity of H_2O_2 dosimetry (in seawater) in comparison to the KI dosimetry. The lower H_2O_2 production in seawater (compared to distilled water) is explained by the scavenging effects towards •OH and Cl• radicals (Reactions (5), (7), (8), and (12)) and H_2O_2 (Reactions (23)-(25)). However, the impact of reducing the gas concentration has conflicting effects (reduces the nucleus number and at the same time reduces the coalescence and attenuation phenomena), which require more investigation.

3.4. Fricke dosimetry

As it can be seen in Fig. 5(a), the yield of Fe^{3+} goes up with the rise in electric power (from 20 to 80 W) for seawater and distilled water. The confrontation of Fe^{3+} concentration in both mediums shows some fluctuation in the production of ferric ions over the sono-irradiation time

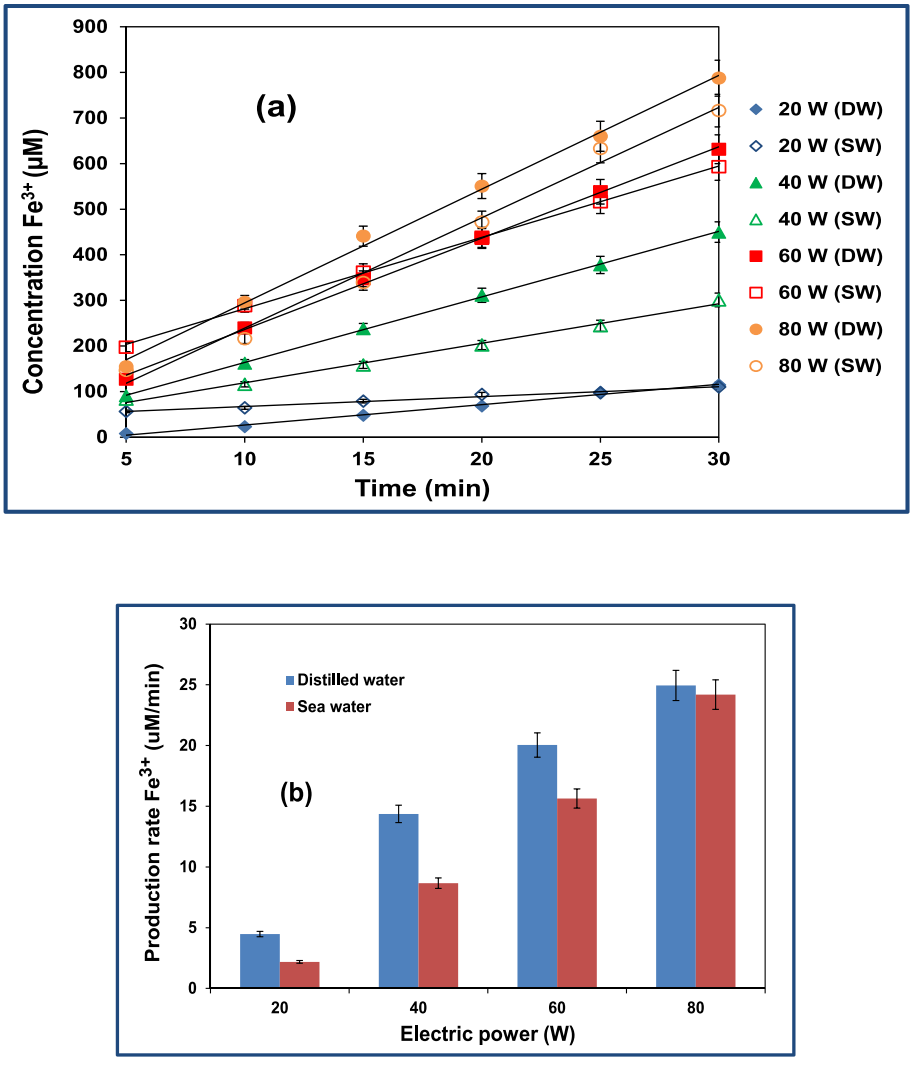

Fig. 5. Temporal variation of ferric ions concentration (a) and its production rate (b) for the same conditions as in Fig. 2. (for (a): $R^2 > 0.98$).

(30 min), this is especially at 20 and 40 W. However, according to Fig. 5 (b), the production rate of ferric ions in distilled water is always higher than that in seawater. For example, at 20 and 80 W, respectively, the production rate of Fe^{3+} in distilled water is 2.04 and 1.03 times higher than that obtained for seawater. In general, the gap between the obtained results in both mediums is reduced with the increase in the electric power (from 20 to 80 W), as shown in Fig. 5(b). The decrease in Fe^{3+} formation is mainly ascribed to the different scavenging reactions causing the elimination of the oxidants (•OH, HO_2•, and H_2O_2) responsible for Fe^{2+} oxidation [Reactions (5), (8), (17), (20), (21), (23)-(25)]. These inhibiting processes are mainly ensured by chloride and bromide ions scattered in seawater. Additionally, the concentration of Fe^{2+} and its oxidation rate are plausibly reduced due to the attack of chlorine species [75,78]:

$$Fe^{2+} + Cl^- \leftrightarrow FeCl^+ \quad k_{26} = 2.88 \times 10^{10} M^{-1}s^{-1},\ k_{-26} = 1 \times 10^{10} M^{-1}s^{-1} \tag{26}$$

$$Fe^{2+} + Cl^{\cdot} \leftrightarrow Cl^- + Fe^{3+} \quad k_{27} = 5.9 \times 10^{9} M^{-1}s^{-1} \tag{27}$$

$$Fe^{2+} + Cl_2^- \rightarrow 2Cl^- + Fe^{3+} \quad k_{28} = 5 \times 10^{6} M^{-1}s^{-1} \tag{28}$$

$$FeCl^+ + H_2O_2 \rightarrow Cl^- + Fe^{3+} + \cdot OH + {}^-OH \quad k_{29} = 55 M^{-1}s^{-1} \tag{29}$$

$$FeCl^+ + HO_2^{\cdot} \rightarrow HO_2^- + Fe^{3+} + Cl^- \quad k_{30} = 1.2 \times 10^{6} M^{-1}s^{-1} \tag{30}$$

In turn, the yield of ferric ions is reduced due to the formation of Fe(II) and Fe(III)-chlorocomplexes ($FeCl^+$, $FeCl^{2+}$, $FeCl_2^+$…), reactions (26)-(32). These complexes could be attacked by HO_2• and O_2•$^-$ [75], whereas this mechanism (decomposition by HO_2• and O_2•$^-$) is not expected to be important under the adopted acoustical conditions.

$$Fe^{3+} + Cl^- \leftrightarrow FeCl^{2+} \quad k_{31} = 6.61 \times 10^{10} M^{-1}s^{-1},\ k_{-31} = 1 \times 10^{10} M^{-1}s^{-1} \tag{31}$$

$$Fe^{3+} + 2Cl^- \leftrightarrow FeCl_2^+ \quad k_{32} = 1.05 \times 10^{11} M^{-1}s^{-1},\ k_{-32} = 1 \times 10^{10} M^{-1}s^{-1} \tag{32}$$

In addition to the scavenging mechanism of Cl^- and Br^- towards •OH, H_2O_2, Fe^{2+}, and Fe^{3+} (Reactions (5)-(32)), sulfate ions (3 g/L in seawater, Table 2) play an important role in reducing Fricke dosimetry efficiency. In the experimental work of De Laat et al. [78], a drastic decrease in the decomposition of H_2O_2 with Fe_3^+ and the oxidation of organic compounds such as atrazine, 4-nitrophenol, and acetic acid in the Fe^{3+}/H_2O_2 system, was observed in the presence of SO_4^{2-} (33.33 mM) and Cl^- (100 mM) compared to NO_3^- (100 mM) and ClO_4^- (100 mM). This behavior was ascribed to the complexation of Fe(III) by Cl^- ($FeCl^+$, $FeCl^{2+}$, $FeCl_2^+$…) and SO_4^{2-} ($FeSO_4^+$, $Fe(SO_4)_2^-$) [79,80], despite of this, it has been suggested that chlorine and sulfate radicals (involved in the degradation process) are generated in the presence of Cl^- and SO_4^{2-} (chlorine and sulfate radicals are less reactive than •OH) [75,78]. The negative effect of salts (justified by the formation of iron(III)-chloro (and sulfate) complexes and scavenging of •OH by chloride) was also obtained by Bandala et al. [10] for the UV/Fenton process, where the degradation of Domic acid (DA) was drastically decreased in seawater compared to the deionized water. In contrast, according to De Laat et al. [78], the oxidation of Fe_2^+ with H_2O_2 was relatively accelerated in the presence of SO_4^{2-} compared to ClO_4^-, NO_3^-, and Cl^-. The same outcomes were retrieved by Orozco et al. [79] for the decomposition of H_2O_2 in the presence of different ferric and ferrous salts. According to these results, it can be clearly retrieved that the presence of Cl^-, Br^-, and SO_4^{2-} has a clear adverse effect on the Fricke dosimetry, especially at low electric power (i.e. 20 and 40 W). The obtained performance of Fricke dosimetry in seawater is the translation of the competitive effects (enhancing and inhibiting roles) of the diverse salts present in seawater. However, with the increase in electric power, very close findings for Fricke dosimetry are retrieved from both mediums. This indicates that the negative effects of salts are reduced at higher acoustic powers.

3.5. 4-Nitrophenol (4-NP) dosimetry

In Fig. 6(a), the evolution of 4-nitrocatechol (4-NC) concentration is shown over the irradiation time (30 min) for seawater and distilled water at each electric power (20–80 W). The production rate of 4-NC (an indicator of 4-NP decay) is depicted in Fig. 6(b). As can be seen in Fig. 6 (a), at 20 W, seawater is dominant in terms of 4-NC production over the irradiation phase (30 min), whereas, with the raise in the electric power from 20 to 80 W, this dominance is gradually shifted towards distilled water. However, in both mediums, the yield of 4-NC goes up with the increase in the electric power. On the other side [Fig. 6(b)], approximately the same formation rate of 4-NC is retrieved for both mediums at 20 W. However, higher production rates of 4-NC are obtained for distilled water (compared to seawater) for the electric power greater than 20 W. Before explaining these findings, a brief analysis should be conducted to explain the effects of the sonicated medium on the 4-NP decomposition.

In general, 4-NP is oxidized via hydrogen abstraction reaction that involves the electrophilic attack of hydroxyl radical ($k = 3.8 \times 10^9$ $M^{-1}s^{-1}$ [81]) at the ortho position of the benzene ring (to a minor extent, •OH-addition takes place in *para*-position) [82,83]. In alkaline conditions, 4-NP (pKa = 7.1) is mainly found under the non-volatile 4-nitrophenolate ionic form (a hydrophilic and deprotonated form of 4-NP [82]), which is responsible for the high •OH scavenging kinetic ($k = 7.6 \times 10^9$ M^{-1} s^{-1} [81]) at this level. However, in acidic conditions, oxidative-pyrolytic pathway of 4-NP (volatile scavenger [84]) in the gaseous phase (within the bubble) and at the interfacial region of bubbles is dominant [82,85]. This effect is promoted with the increase of 4-NP hydrophobicity giving an enrichment of about 80 times higher (at pH 4) than that of the 4-nitrophenolate ion (at pH 10) at the same substrate dose [82]. Additionally, due to the higher solubility of the charged form of 4-NP (65.0 g/L at 25 °C) compared to the uncharged one (11.6 g/L at 20 °C), the uncharged form (neutral form) under the acidic conditions is expected to be favorably pushed towards the hydrophobic bubble/water interface [86]. This is in addition to the preliminary evaporation of 4-NP molecules inside bubbles. It should be noted that the importance of the pyrolytic decomposition of 4-NP was corroborated via the considerable yield (~88 % of the total production) of the thermolysis products (such as CO, CO_2, phenol, nitrate, and H_2) of 4-NP (Log $P_{Octanol/water} = 2.04$ [84]) sonolysis at low pH [82].

In the present study, the existence of the ionic form of 4-NP (4-nitrophenolate) is not expected to be important; because all the sonoirradiations were carried out in a neutral medium, Table 2. Therefore, at a constant electric power and at the beginning of the irradiation time [Fig. 6 (a), (b)], 4-NP is mainly oxidized by •OH radicals in the surrounding liquid. However, as time elapses, the solution pH goes down, thus, the degradation of 4-NP (via pyrolysis and •OH attacks) is gradually shifted towards the bubble/liquid interface and the bubble interior. The decomposition of 4-NP is even boosted with the increase in the electric power due to the decrease in solution pH thanks to the formation of nitric and nitrous acids [76,87–89]. The positive effect of pH reduction on 4-Nitrophenol decay has been observed in many experimental works [82,85,86,90]. Nevertheless, according to Al-Juboori et al. [83], with the use of ½" probe, the variation of pH (4 and 10) has no effect on the 4-NC yield, whereas, using a ¾" probe, the formation of 4-NC goes down at pH 10 (as a function of the irradiation time: 5, 10, and 15 min) compared to pH 4. However, contrary to our study, for both probes (½" and ¾") the decomposition rate of 4-NP was amortized with the increase in the ultrasound power. This discrepancy is ascribed to the different operating conditions adopted in our work (300 kHz, $P_E = 20$, 40, 60, 80 W) compared to those of Al-Juboori et al. (20 kHz, $P_{E,max,1/2''} = 112.5$ W, $P_{E,max,3/4''} = 180$ W).

In addition to the positive effect of low solution pH, the degradation of 4-NP is expected to be promoted in seawater, because in the presence

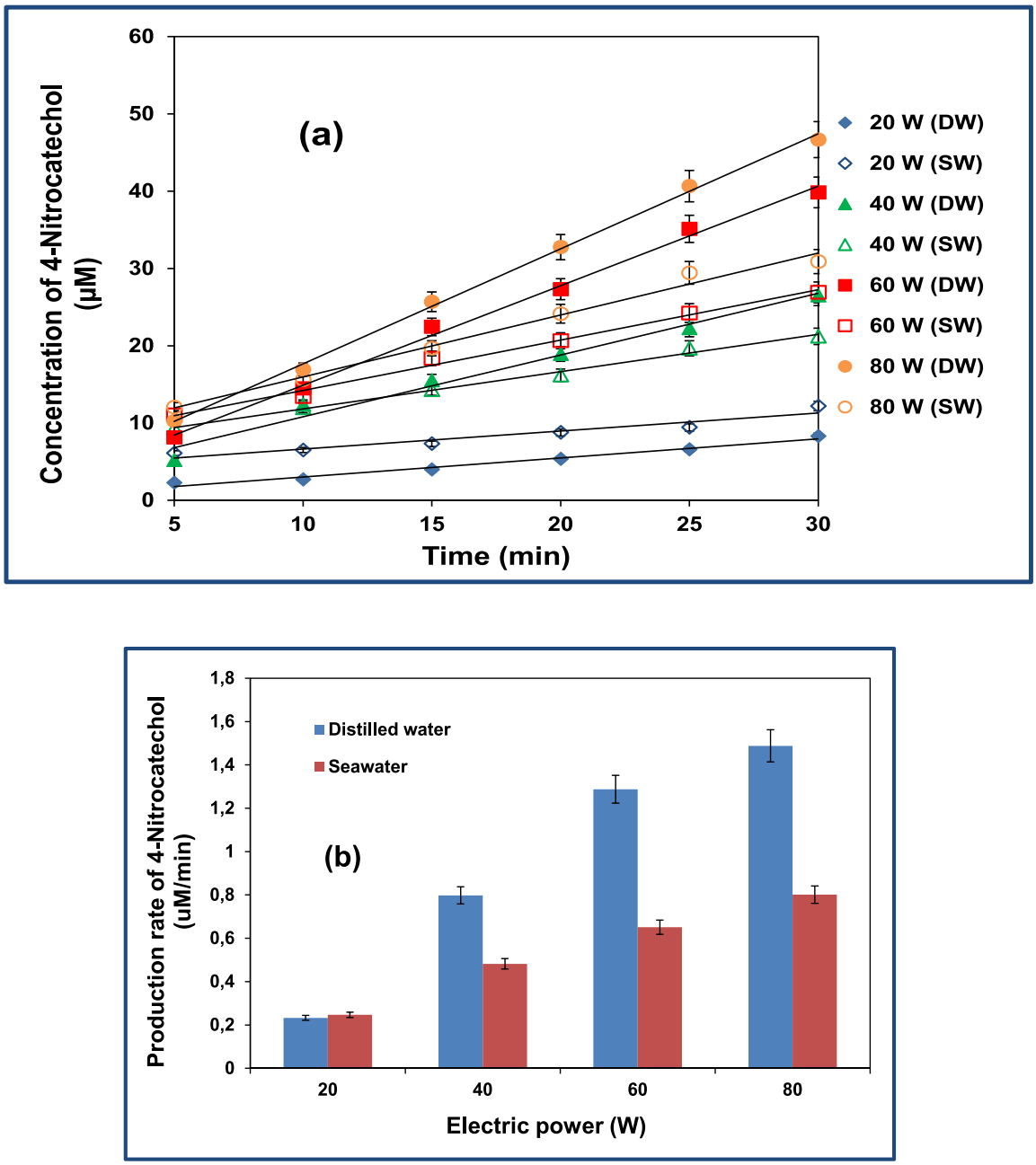

Fig. 6. Temporal variation of 4-Nitrocatechol concentration (a) and its production rate (b) for the same conditions as in Fig. 2. (for (a): $R^2 > 0.99$).

of different salts (Table 2), the hydrophobicity of 4-NP goes up with the increase in aqueous phase hydrophilicity (partitioning coefficient goes up [11]). Consequently, 4-NP molecules are pushed from the bulk solution towards the hot bubble interface (in addition to the 4-NP molecules entering the bubble during the rarefaction phase). As a result, the possibility of •OH radicals attack and the pyrolytic decomposition of 4-NP are improved in the presence of various salts. This result is supported by the experimental investigation of Guo et al. [91] for the sono-conversion efficiency of 2,4-dinitrophenol (DNP) using US/H_2O_2/NaCl process ($[NaCl]_0 = 0.1$ M), where an enhancement of 1.3-times was obtained compared to that without NaCl. In the experimental work of Gogate et al. [92], an enhancement of almost five times was retrieved for the sono-removal rate of phenol in the presence of NaCl (8 %). This was explained by the increase in the partitioning (pollutant molecules are accumulated at the implosion sites), decrease in vapor pressure as well as the increase in surface tension (harshening the bubble collapse) in the presence of NaCl. Interestingly, according to the experimental study of Mahamuni and Pandit [93], it was concluded that phenol molecules are only affected by the salting-out mechanism applied by NaCl, whereas, no involvement of this latter was observed in the degradation process of phenol (confirmed via the decomposition products).

According to the foregoing discussion and with the consideration of the positive impacts of pH and the salting-out effect, it seems that other factors are participating in the observed behaviors in Fig. 6(a), (b). As a result, at an electric power of 20 W, it seems that for seawater, the positive effects of pH decrease and salting-out mechanism override the decrease in number density, the generation of small bubbles and the scavenging effects of Cl^- and Br^- (discussed in the previous sections) for •OH radicals, this in addition to the relatively low conversion of 4-NP in distilled water. Therefore, higher production is observed in this case compared to that of distilled water. Despite of that, as can be seen in Fig. 6(b), approximately the same production rates are retrieved for both

mediums. In contrast, as the electric power goes up (>20 W), as shown in Fig. 6(a), the yield of 4-NC in distilled water is substantially enhanced, whereas, in seawater, the generation of relatively small bubbles (compared to distilled water) affects negatively the formation of 4-NC. Consequently, despite the improving effect of pH and the salting-out process (for $P_E > 20$), the negative impacts of small bubbles and •OH scavenging (via Cl^- and Br^-) in seawater seem to be dominant. As a result, higher production rates of 4-NC are obtained for distilled water compared to seawater in the case of $P_E > 20$ W, as shown in Fig. 6(b). The obtained findings of Fig. 6(a) and 6(b) show the effectiveness of using 4-NP sonoconversion for the evaluation of the sonochemical activity during the irradiation of seawater and distilled water.

3.6. Ascorbic acid dosimetry

Due to its high capacity for scavenging hydroxyl radicals [94,95], ascorbic acid (AA) has been selected to monitor the sonochemical activity in seawater and distilled water over an irradiation time of 30 min and for electric power ranging from 20 to 80 W, as shown in Fig. 7. It should be noted that Ascorbic acid (AA or Vc) is well known for its preferential reaction with •OH radicals ($k_{OH+AA} = 1.2 \times 10^{10}\ M^{-1}\ s^{-1}$). For example, more than 95 % of •OH (formation of $H_2O_2 \approx 0$) was quenched in the presence of 10 mM of ascorbic acid (at 358 kHz, 0.9 W/cm^2) compared to the 50 % of inhibition in the presence of ethanol (volatile quencher) [32]. Moreover, AA may be used for the generation of •OH radicals (oxidation enhancer) via the reduction of Fe(III) and O_2 to generate Fe(II) and H_2O_2 (Fenton reactants), respectively [96]. Furthermore, the generation of •OH radicals is possibly increased in the presence of H_2O_2/AA system [97–99], or even enhanced by the synergistic process with ultrasound irradiation (H_2O_2/AA/US) [98] and microwave irradiation (MW/AA/H_2O_2) [100]. Additionally, AA is a satisfactory scavenging (reducing agent) means for the residual active (oxidizing) chlorine species (for the fixation of the chlorination byproducts) [101,102].

In contrast to the high reactivity of AA with hydroxyl radicals ($k_{OH+AA} = 1.2 \times 10^{10}\ M^{-1}\ s^{-1}$), a relatively lower hydrophobicity is exhibited by ascorbic acid in comparison to phenol [32]. Additionally, a relatively high solubility is retrieved for AA in water compared to the other polar solvents (ethanol, methanol…) [103]. Despite of that, it is expected that the higher reactivity of AA (with •OH radicals) in addition to the positive effect of the salting-out process are the controlling parameters for the probing mechanism of ascorbic acid in both mediums.

At first sight, from Fig. 7, it can be retrieved that practically no difference is observed for the degradation of AA (normalized concentration) in both mediums (SW and DW), where the decomposition rate increased with the raise in the electric power (from 20 to 80 W). The obtained findings of Fig. 7 clearly indicate that the decomposition mechanism is not affected by the composition of the irradiated medium (seawater or distilled water). The performance of the probing mechanism seems to be similar to that using potassium iodide [Fig. 3 (a) and (b)]. As a result, ascorbic acid could be used with high confidence as a probing agent for the monitoring of the sonochemical activity in the sonicated medium.

4. Conclusion

For an ultrasound frequency of 300 kHz, the performance of calorimetry, KI, Fricke, H_2O_2, 4-nitrophenol, and acid ascorbic dosimetry methods has been investigated by spanning the electric power (P_E) range from 20 to 80 W. This study was carried out for seawater and distilled water.

Compared to distilled water, it has been obtained that the lowest temperatures and calorimetric energies were retrieved for seawater for all the applied electric powers. Nevertheless, with the raise in the electric power up to 80 W, the discrepancy between both mediums is reduced.

Due to the lesser effect of the salty composition of seawater (compared to distilled water) on the performance of KI and ascorbic acid dosimetries (especially at higher P_E), these techniques could be used with confidence for an efficient probing of the sono-irradiated solution activity.

In contrast, independently of the applied electric power (from 20 to 80 W), the H_2O_2 dosimetry was negatively influenced by seawater matrice (compared to distilled water).

At 20 and 40 W, the performance of Fricke dosimetry was substantially influenced by the composition of seawater (compared to distilled water), whereas, with the increase of electric power up to 80 W, the adverse effect of seawater was amortized with a similar performance of the Fricke dosimetry in both mediums. The opposite behavior was retrieved for the 4-NP dosimetry, where a lower performance is observed in seawater for the electric power higher than 20 W.

Taking into account the performance of each of the investigated methods, it can be indicated that the analyzed dosimetry techniques could be classified in the following order: Ascorbic acid ≈ KI > Fricke > 4-nitrophenol > H_2O_2. As a result, ascorbic acid and KI dosimetries are regarded as reliable approaches for an efficient evaluation of the sonochemical activity in a sonicated solution.

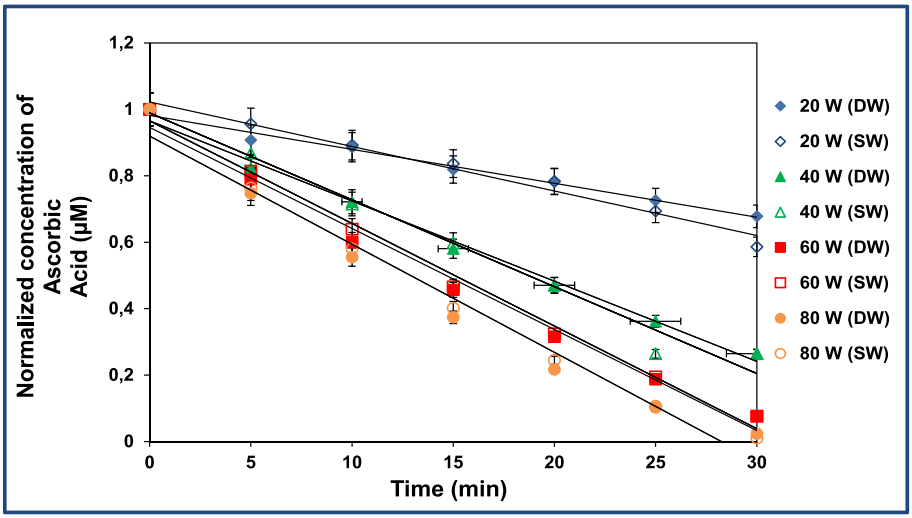

Fig. 7. Temporal evolution of the normalized concentration of ascorbic acid under the same conditions of Fig. 2. ($R^2 > 0.97$).

Declaration of Competing Interest

The authors declare that they have no known competing financial interests or personal relationships that could have appeared to influence the work reported in this paper.

Data availability

No data was used for the research described in the article.

Acknowledgments

The authors extend their appreciation to the Deputyship for Research and Innovation, "Ministry of Education" in Saudi Arabia for funding this research (IFKSUOR3–384–1).

References

[1] Y. Yao, Q. Chen, Z. Huang, J. Zhou, Catalytic activity comparison of typical iron-bearing particle electrodes in heterogeneous electro-Fenton oxidation processes, Environ. Technol. Innov. 21 (2021) 101321, https://doi.org/10.1016/j.eti.2020.101321.
[2] F.Z. Meghlaoui, S. Merouani, O. Hamdaoui, M. Bouhelassa, M. Ashokkumar, Rapid catalytic degradation of refractory textile dyes in Fe(II)/chlorine system at near neutral pH: Radical mechanism involving chlorine radical anion ($Cl_2^{\bullet-}$)-mediated transformation pathways and impact of environmental matrices, Sep. Purif. Technol. 227 (2019), 115685, https://doi.org/10.1016/j.seppur.2019.115685.
[3] H. Che, S. Bae, W. Lee, Degradation of trichloroethylene by Fenton reaction in pyrite suspension, J. Hazard. Mater. 185 (2011) 1355–1361, https://doi.org/10.1016/j.jhazmat.2010.10.055.
[4] O. Hamdaoui, S. Merouani, M. Ait, H.C. Benmahmoud, A. Dehane, A. Alghyamah, Ultrasound/chlorine sono-hybrid-advanced oxidation process: Impact of dissolved organic matter and mineral constituents, Ultrason. Sonochem. 83 (2022), 105918, https://doi.org/10.1016/j.ultsonch.2022.105918.
[5] P. Villegas-Guzman, J. Silva-Agredo, A.L. Giraldo-Aguirre, O. Flórez-Acosta, C. Petrier, R.A. Torres-Palma, Enhancement and inhibition effects of water matrices during the sonochemical degradation of the antibiotic dicloxacillin, Ultrason. Sonochem. 22 (2015) 211–219, https://doi.org/10.1016/j.ultsonch.2014.07.006.
[6] E.A. Serna-galvis, J. Porras, R.A. Torres-palma, A critical review on the sonochemical degradation of organic pollutants in urine, seawater, and mineral water, Ultrason. Sonochem. 82 (2022), 105861, https://doi.org/10.1016/j.ultsonch.2021.105861.
[7] M. Wall, M. Ashokkumar, R. Tronson, F. Grieser, Multibubble sonoluminescence in aqueous salt solutions, Ultrason. Sonochem. 6 (1999) 7–14, https://doi.org/10.1016/S1350-4177(98)00037-6.
[8] M. Hamida, A. Dehane, S. Merouani, O. Hamdaoui, M. Ashokkumar, The role of reactive chlorine species and hydroxyl radical in the ultrafast removal of Safranin O from wastewater by CCl_4/ultrasound sono-process, Chem. Eng. Process. - Process Intensif. 178 (2022), 109014, https://doi.org/10.1016/j.cep.2022.109014.
[9] I. Vallés, L. Santos-Juanes, A.M. Amat, J. Moreno-Andrés, A. Arques, Effect of salinity on UVA-vis light driven photo-fenton process at acidic and circumneutral pH, Water 13 (2021) 1315, https://doi.org/10.3390/w13091315.
[10] E.R. Bandala, L. Brito, M. Pelaez, Degradation of domoic acid toxin by UV-promoted Fenton-like processes in seawater, Desalination 245 (2009) 135–145, https://doi.org/10.1016/j.desal.2008.06.015.
[11] J.D. Seymour, R.B. Gupta, Oxidation of Aqueous Pollutants Using Ultrasound : Salt-Induced Enhancement, Ind. Eng. Chem. Res. 36 (1997) 3453–3457, https://doi.org/10.1021/ie970069o.
[12] E.A. Serna-galvis, D. Montoya-rodríguez, L. Isaza-pineda, M. Ibá, F. Hernández, A. Moncayo-lasso, R.A. Torres-Palma, Sonochemical degradation of antibiotics from representative classes- Consid- erations on structural effects, initial transformation products, antimicrobial activity and matrix, Ultson. Sonochem. 50 (2018) 157–165, https://doi.org/10.1016/j.ultsonch.2018.09.012.
[13] O. Hamdaoui, S. Merouani, Impact of seawater salinity on the sonochemical removal of emerging organic pollutants, Environ. Technol. 41 (2020) 2305–2313, https://doi.org/10.1080/09593330.2018.1564071.
[14] S. Boutemedjet, O. Hamdaoui, S. Merouani, C. Pétrier, Sonochemical degradation of endocrine disruptor propylparaben in pure water, natural water, and seawater, Desalin. Water Treat. 57 (2016) 27816–27826, https://doi.org/10.1080/19443994.2016.1177600.
[15] S. Koda, A standard method to calibrate sonochemical efficiency of an individual reaction system, Ultson. Sonochem. 10 (2003) 149–156, https://doi.org/10.1016/S1350-4177(03)00084-1.
[16] Z. Wei, L.K. Weavers, Combining COMSOL Modeling with Acoustic Pressure Maps to Design Sono-reactors, Ultrason. Sonochem. 31 (2016) 490–498, https://doi.org/10.1016/j.ultsonch.2016.01.036.
[17] Y. Son, M. Lim, J. Khim, L. Kim, M. Ashokkumar, Comparison of calorimetric energy and cavitation energy for the removal of bisphenol-A: the effects of frequency and liquid height, Chem. Eng. J. 183 (2012) 39–45, https://doi.org/10.1016/j.cej.2011.12.016.
[18] A. Kumar, S.N. Chatterjee, B. Division, Estimation of hydroxyl free radicals produced by ultrasound in Fricke solution used as a chemical dosimeter, Ultrason. Sonochem. 2 (1995) 87–91, https://doi.org/10.1016/1350-4177(95)00025-2.
[19] D.B. Rajamma, S. Anandan, N.S.M. Yusof, B.G. Pollet, M. Ashokkumar, Sonochemical dosimetry: a comparative study of Weissler, Fricke and terephthalic acid methods, Ultrason. Sonochem. 72 (2021), 105413, https://doi.org/10.1016/j.ultsonch.2020.105413.
[20] S. Merouani, O. Hamdaoui, F. Saoudi, M. Chiha, Influence of experimental parameters on sonochemistry dosimetries: KI oxidation, Fricke reaction and H2O2 production, J. Hazard. Mater. 178 (2010) 1007–1014, https://doi.org/10.1016/j.jhazmat.2010.02.039.
[21] N. Kerabchi, S. Merouani, O. Hamdaoui, Liquid depth effect on the acoustic generation of hydroxyl radical for large scale sonochemical reactors, Sep. Purif. Technol. 206 (2018) 118–130, https://doi.org/10.1016/j.seppur.2018.05.039.
[22] N. Kerabchi, S. Merouani, O. Hamdaoui, Depth effect on the inertial collapse of cavitation bubble under ultrasound: special emphasis on the role of the wave attenuation, Ultson. Sonochem. 48 (2018) 136–150, https://doi.org/10.1016/j.ultsonch.2018.05.004.
[23] H. Ferkous, S. Merouani, O. Hamdaoui, Sonolytic degradation of naphthol blue black at 1700 kHz: effects of salts, complex matrices and persulfate, J. Water Process Eng. 9 (2016) 67–77, https://doi.org/10.1016/j.jwpe.2015.11.003.
[24] D.T. Jamieson, J.S. Tudhope, R. Morris, G. Cartwright, Physical properties of sea water solutions: heat capacity, Desalination 7 (1969) 23–30, https://doi.org/10.1016/S0011-9164(00)80271-4.
[25] I.J. Ave, L. Xincheng, Heat capacity of seawater solutions from 5° to 35°C and 0.5 to 22‰ chlorinity, J. Geophys. Res. 78 (1973) 4–6, https://doi.org/10.1029/JC078i021p04499.
[26] A. Ebrahiminia, M. Mokhtari-Dizaji, T. Toliyat, Dual frequency cavitation event sensor with iodide dosimeter, Ultrason. Sonochem. 28 (2016) 276–282, https://doi.org/10.1016/j.ultsonch.2015.07.005.
[27] C. Kormann, D.W. Bahnemann, M.R. Hoffmann, Photocatalytic production of hydrogen peroxides and organic peroxides in aqueous suspensions of titanium dioxide, zinc oxide, and desert sand, Environ. Sci. Tech. 22 (1988) 798–806, https://doi.org/10.1021/es00172a009.
[28] H. Nomura, S. Koda, K. Yasuda, Y. Kojima, Quantification of ultrasonic intensity based on the decomposition reaction of porphyrin, Ultrason. Sonochem. 3 (1996) 3–6, https://doi.org/10.1016/S1350-4177(96)00020-X.
[29] C. Pdtrier, A. Francony, Ultrasonic waste-water treatment: incidence of ultrasonic frequency on the rate of phenol and carbon tetrachloride degradation, Ulrason. Sonochem. 4 (1997) 295–300, https://doi.org/10.1016/S1350-4177(97)00036-9.
[30] C. Petrier, A. Francony, Incidence of wave-frequency on the reaction rates during ultrasonic wastewater treatment, Wat. Sci. Tech. 35 (1997) 175–180, https://doi.org/10.1016/S0273-1223(97)00023-1.
[31] H. Ferkous, O. Hamdaoui, C. Pétrier, Sonochemical formation of peroxynitrite in water: impact of ultrasonic frequency and power, Ultrason. Sonochem. 98 (2023) 106488, https://doi.org/10.1016/j.ultsonch.2023.106488.
[32] M. Ashokkumar, D. Sunartio, S. Kentish, R. Mawson, L. Simons, K. Vilkhu, C. (Kees) Versteeg, Modification of food ingredients by ultrasound to improve functionality: a preliminary study on a model system, Innov. Food Sci. Emerg. Technol. 9 (2008) 155–160, https://doi.org/10.1016/j.ifset.2007.05.005.
[33] M.W. Davey, G. Bauw, M. Van Montagu, Analysis of ascorbate in plant tissues by high-performance capillary zone electrophoresis, Anal. Biochem. 239 (1996) 8–19, https://doi.org/10.1006/abio.1996.0284.
[34] R.J. Wood, J. Lee, M.J. Bussemaker, Combined effects of flow, surface stabilisation and salt concentration in aqueous solution to control and enhance sonoluminescence, Ultrason. Sonochem. 58 (2019) 104683, https://doi.org/10.1016/j.ultsonch.2019.104683.
[35] A. Dehane, S. Merouani, A. Chibani, O. Hamdaoui, K. Yasui, M. Ashokkumar, Estimation of the number density of active cavitation bubbles in a sono-irradiated aqueous solution using a thermodynamic approach, Ultrasonics 126 (2022), 106824, https://doi.org/10.1016/j.ultras.2022.106824.
[36] T. Tuziuti, K. Yasui, M. Sivakumar, Y. Iida, Correlation between Acoustic Cavitation Noise and Yield Enhancement of Sonochemical Reaction by Particle Addition, Chem. A Eur. J. 109 (2005) 4869–4872, https://doi.org/10.1021/jp0503516.
[37] Y. Son, M. Lim, M. Ashokkumar, J. Khim, Geometric Optimization of Sonoreactors for the Enhancement of Sonochemical Activity, J. Phys. Chem. 115 (2011) 4096–4103, https://doi.org/10.1021/jp110319y.
[38] M. Toma, S. Fukutomi, Y. Asakura, S. Koda, A calorimetric study of energy conversion efficiency of a sonochemical reactor at 500 kHz for organic solvents, Ultrason. Sonochem. 18 (2011) 197–208, https://doi.org/10.1016/j.ultsonch.2010.05.005.
[39] S. Koda, T. Kimura, T. Kondo, H. Mitome, A standard method to calibrate sonochemical efficiency of an individual reaction system, Ulrason. Sonochem. 10 (2003) 149–156, https://doi.org/10.1016/S1350-4177(03)00084-1.
[40] J. David, N. Cheeke, Fundamentals and applications of ultrasonic waves, CRC Press LLC, 2002.
[41] L.E. Kinsler, A.R. Frey, A.B. Copens, J.V. Sanders, Fundamentals of Acoustics, Fourth Edition, John Wiley & Sons, 2000.
[42] T.J. Mason, J.P. Lorimer, Applied Sonochemistry: Uses of Power Ultrasound in Chemistry and Processing, Wiley-VCH Verlag GmbH & Co. KGaA, Weinheim, Gu, 2002.

[43] S. Muthukumaran, S.E. Kentish, G.W. Stevens, M. Ashokkumar, Application of ultrasound in membrane separation processes: A review, Rev. Chem. Eng. 22 (2006) 155–194. https://doi.org/10.1515/REVCE.2006.22.3.155.
[44] A. Dehane, S. Merouani, O. Hamdaoui, Chapter 9 - Energy controlling mechanisms: Relationship with operational conditions, in: O. Hamdaoui, K. Kerboua (Eds.), Energy Aspects of Acoustic Cavitation and Sonochemistry: Fundamentals and Engineering, Elsevier, 2022, pp. 145–155. https://doi.org/10.1016/B978-0-323-91937-1.00007-4.
[45] A. Dehane, S. Merouani, O. Hamdaoui, Chapter 2 - The energy forms and energy conversion, in: O. Hamdaoui, K. Kerboua (Eds.), Energy Aspects of Acoustic Cavitation and Sonochemistry: Fundamentals and Engineering, Elsevier, 2022, pp. 23–35, https://doi.org/10.1016/B978-0-323-91937-1.00012-8.
[46] A. Brotchie, T. Statham, M. Zhou, L. Dharmarathne, F. Grieser, M. Ashokkumar, Acoustic Bubble Sizes, Coalescence, and Sonochemical Activity in Aqueous Electrolyte Solutions Saturated with Different Gases, Langmuir 26 (2010) 12690–12695, https://doi.org/10.1021/la1017104.
[47] R. Pflieger, J. Lee, S.I. Nikitenko, M. Ashokkumar, Influence of He and Ar Flow Rates and NaCl Concentration on the Size Distribution of Bubbles Generated by Power Ultrasound, J. Phys. Chem. B 119 (2015) 12682–12688, https://doi.org/10.1021/acs.jpcb.5b08723.
[48] T. Tuziuti, K. Yasui, Y. Iida, M. Sivakumar, S. Koda, Laser-Light Scattering from a Multibubble System for Sonochemistry, Chem. A Eur. J. 108 (2004) 9011–9013, https://doi.org/10.1021/jp046758c.
[49] T. Tuziuti, K. Yasui, K. Kato, Influence of Degree of Gas Saturation on Multibubble Sonoluminescence Intensity, Chem. A Eur. J. 115 (2011) 5089–5093, https://doi.org/10.1021/jp201473q.
[50] J. Lee, S.E. Kentish, M. Ashokkumar, The Effect of Surface-Active Solutes on Bubble Coalescence in the Presence of Ultrasound, J. Phys. Chem. B 109 (2005) 5095–5099, https://doi.org/10.1021/jp0476444.
[51] R. Pflieger, S.I. Nikitenko, M. Ashokkumar, Effect of NaCl salt on sonochemistry and sonoluminescence in aqueous solutions,, Ultson. Sonochem. 59 (2019) 104753, https://doi.org/10.1016/j.ultsonch.2019.104753.
[52] T.G. Leighton, What is ultrasound? Prog. Biophys. Mol. Biol. 93 (2007) 3–83, https://doi.org/10.1016/j.pbiomolbio.2006.07.026.
[53] R.J. Wood, J. Lee, M.J. Bussemaker, A parametric review of sonochemistry: control and augmentation of sonochemical activity in aqueous solutions, Ultson. Sonochem. 38 (2017) 351–370, https://doi.org/10.1016/j.ultsonch.2017.03.030.
[54] Y. Shen, K. Yasui, T. Zhua, M. Ashokkumar, A model for the effect of bulk liquid viscosity on cavitation bubble dynamics, Phys. Chem. Chem. Phys. 19 (2017) 20635–20640, https://doi.org/10.1039/C7CP03194G.
[55] H. Nazari-Mahroo, K. Pasandideh, H.A. Navid, R. Sadighi-Bonabi, How important is the liquid bulk viscosity effect on the dynamics of a single cavitation bubble? Ultrason. Sonochem. 49 (2018) 47–52, https://doi.org/10.1016/j.ultsonch.2018.07.013.
[56] J. Holzfuss, Acoustic energy radiated by nonlinear spherical oscillations of strongly driven bubbles, Proc. R. Soc. A 466 (2010) 1471–2946, https://doi.org/10.1098/rspa.2009.0594.
[57] K. Yasui, T. Tuziuti, W. Kanematsu, Extreme conditions in a dissolving air nanobubble, Phys. Rev. E 94 (2016) 013106. https://doi.org/10.1103/PhysRevE.94.013106.
[58] P.R. Gogate, S.N. Katekhaye, A comparison of the degree of intensification due to the use of additives in ultrasonic horn and ultrasonic bath, Chem. Eng. Process. 61 (2012) 23–29, https://doi.org/10.1016/j.cep.2012.06.016.
[59] S.N. Katekhaye, P.R. Gogate, Intensification of cavitational activity in sonochemical reactors using different additives: efficacy assessment using a model reaction, Chem. Eng. Process. 50 (2011) 95–103, https://doi.org/10.1016/j.cep.2010.12.002.
[60] M. Gutiérrez, A. Henglein, H. Mockel, Observations on the role of MgCl2 in the Weissler reaction, Ultrason. Sonochem. 2 (1995) 1994–1996, https://doi.org/10.1016/1350-4177(94)00005-D.
[61] T. Lepoint, F. Mullie, What exactly is cavitation chemistry? Ultrason. Sonochem. 1 (1994) 13–22, https://doi.org/10.1016/1350-4177(94)90020-5.
[62] F.C. Kracek, The solubility of potassium iodide in water to 240°, J. Phys. Chem. 35 (1931) 947–949, https://doi.org/10.1021/j150322a002.
[63] L. Sanchez-prado, R. Barro, C. Garcia-jares, M. Llompart, M. Lores, C. Petrakis, N. Kalogerakis, D. Mantzavinos, Sonochemical degradation of triclosan in water and wastewater, Ultrason. Sonochem. 15 (2008) 689–694, https://doi.org/10.1016/j.ultsonch.2008.01.007.
[64] A. Taamallah, S. Merouani, O. Hamdaoui, Sonochemical degradation of basic fuchsin in water, Desalin. Water Treat. 57 (2016) 27314–27330, https://doi.org/10.1080/19443994.2016.1168320.
[65] H. Uddin, B. Nanzai, K. Okitsu, Effects of Na2SO4 or NaCl on sonochemical degradation of phenolic compounds in an aqueous solution under Ar: positive and negative effects induced by the presence of salts, Ultrason. Sonochem. 28 (2016) 144–149, https://doi.org/10.1016/j.ultsonch.2015.06.028.
[66] N.E. Chadi, S. Merouani, O. Hamdaoui, M. Bouhelassa, M. Ashokkumar, Influence of mineral water constituents, organic matter and water matrices on the performance of the H2O2/IO4−-advanced oxidation process, Environ. Sci. Water Res. Technol. 5 (2019) 1985–1992, https://doi.org/10.1039/c9ew00329k.
[67] A. Belghit, S. Merouani, O. Hamdaoui, M. Bouhelassa, S. Al-Zahrani, The multiple role of inorganic and organic additives in the degradation of reactive green 12 by UV/chlorine advanced oxidation process, Environ. Technol. (united Kingdom) 43 (2022) 835–847, https://doi.org/10.1080/09593330.2020.1807609.
[68] J. Fang, Y. Fu, C. Shang, The roles of reactive species in micropollutant degradation in the UV/free chlorine system, Environ. Sci. Tech. 48 (2014) 1859–1868, https://doi.org/10.1021/es4036094.
[69] T. Yang, J. Mai, S. Wu, C. Liu, L. Tang, Z. Mo, M. Zhang, L. Guo, M. Liu, J. Ma, UV/chlorine process for degradation of benzothiazole and benzotriazole in water: efficiency, mechanism and toxicity evaluation, Sci. Total Environ. 760 (2021), 144304, https://doi.org/10.1016/j.scitotenv.2020.144304.
[70] K. Guo, Z. Wu, J. Fang, UV-based advanced oxidation process for the treatment of pharmaceuticals and personal care products, in: A.J. Hernández-Maldonado, L. Blaney (Eds.), Contam. Emerg, Concern Water Wastewater, Elsevier Inc., 2020, pp. 367–408, https://doi.org/10.1016/B978-0-12-813561-7.00010-9.
[71] Z. Gao, Y. Lin, B. Xu, Y. Xia, C. Hu, T. Zhang, H. Qian, T. Cao, N. Gao, Effect of bromide and iodide on halogenated by-product formation from different organic precursors during UV/chlorine processes, Water Res. 182 (2020) 116035, https://doi.org/10.1016/j.watres.2020.116035.
[72] S. Merouani, O. Hamdaoui, F. Saoudi, M. Chiha, Sonochemical degradation of Rhodamine B in aqueous phase: effects of additives, Chem. Eng. J. 158 (2010) 550–557, https://doi.org/10.1016/j.cej.2010.01.048.
[73] C. Pétrier, R. Torres-Palma, E. Combet, G. Sarantakos, S. Baup, C. Pulgarin, Enhanced sonochemical degradation of bisphenol-A by bicarbonate ions, Ultrason. Sonochem. 17 (2010) 111–115, https://doi.org/10.1016/j.ultsonch.2009.05.010.
[74] S. Bekkouche, S. Merouani, O. Hamdaoui, M. Bouhelassa, Efficient photocatalytic degradation of Safranin O by integrating solar-UV/TiO2/Persulfate treatment: implication of sulfate radical in the oxidation process and effect of various water matrix components, J. Photochem. Photobiol. A Chem. 345 (2017) 80–91, https://doi.org/10.1016/j.jphotochem.2017.05.028.
[75] J. De Laat, T.G. Le, Effects of chloride ions on the iron (III) -catalyzed decomposition of hydrogen peroxide and on the efficiency of the Fenton-like oxidation process, Appl. Catal. B Environ. 66 (2006) 137–146, https://doi.org/10.1016/j.apcatb.2006.03.008.
[76] C.A. Wakeford, R. Blackburn, P.D. Lickiss, Effect of ionic strength on the acoustic generation of nitrite, nitrate and hydrogen peroxide, Ultrason. Sonochem. 6 (1999) 141–148, https://doi.org/10.1016/S1350-4177(98)00039-X.
[77] K. Okitsu, T. Suzuki, N. Takenaka, H. Bandow, R. Nishimura, Y. Maeda, Acoustic multibubble cavitation in water: a new aspect of the effect of a rare gas atmosphere on bubble temperature and its relevance to sonochemistry, J. Phys. Chem. B 110 (2006) 20081–20084, https://doi.org/10.1021/jp064598u.
[78] J. De Laat, G.T. Le, B. Legube, A comparative study of the effects of chloride, sulfate and nitrate ions on the rates of decomposition of H2O2 and organic compounds by Fe(II)/H2O2 and Fe(III)/H2O 2, Chemosphere 55 (2004) 715–723, https://doi.org/10.1016/j.chemosphere.2003.11.021.
[79] S.L. Orozco, E.R. Bandala, C.A. Arancibia-Bulnes, B. Serrano, R. Suárez-Parra, I. Hernández-Pérez, Effect of iron salt on the color removal of water containing the azo-dye reactive blue 69 using photo-assisted Fe(II)/H2O2 and Fe(III)/H2O2 systems, J. Photochem. Photobiol. A Chem. 198 (2008) 144–149, https://doi.org/10.1016/j.jphotochem.2008.03.001.
[80] J. Bacardit, J. Sto, E. Chamarro, S. Esplugas, Effect of Salinity on the Photo-Fenton Process, Ind. Eng. Chem. Res. 46 (2007) 7615–7619, https://doi.org/10.1021/ie070154o.
[81] G.V. Buxton, C.L. Greenstock, W.P. Helman, A.B. Ross, G.V. Buxton, C. L. Greenstock, P. Helman, A.B. Ross, Critical Review of rate constants for reactions of hydrated electrons, hydrogen atoms and hydroxyl radicals (·OH /·O) in Aqueous Solution, J. Phys. Chem. Ref. Data 17 (1988) 513–886, https://doi.org/10.1063/1.555805.
[82] A. Tauber, H.P. Schuchmann, C. Von Sonntag, Sonolysis of aqueous 4-nitrophenol at low and high pH, Ultrason. Sonochem. 7 (2000) 45–52, https://doi.org/10.1016/S1350-4177(99)00018-8.
[83] R.A. Al-Juboori, T. Yusaf, L. Bowtell, V. Aravinthan, Energy characterisation of ultrasonic systems for industrial processes, Ultrasonics 57 (2015) 18–30, https://doi.org/10.1016/j.ultras.2014.10.003.
[84] R.P. Schwarrenbach, R. Stierli, B.R. Folsom, J. Zeyer, Compound Properties Relevant for Assessing the Environmental Partitioning of Nitrophenols, Environ. Sci. Tech. 22 (1988) 83–92, https://doi.org/10.1021/es00166a009.
[85] A. Kotronarou, G. Mills, M.R. Hoffmann, Ultrasonic irradiation of p-nitrophenol in aqueous solution, J. Phys. Chem. 95 (1991) 3630–3638, https://doi.org/10.1021/j100162a037.
[86] Y. Jiang, P. Christian, T.D. Waite, C. Pétrier, T.D. Waite, P. Christian, T.D. Waite, Effect of pH on the ultrasonic degradation of ionic aromatic compounds in aqueous solution, Ultrason. Sonochem. 9 (2002) 163–168, https://doi.org/10.1016/S1350-4177(01)00114-6.
[87] E.L. Mead, R.G. Sutherland, R.E. Verrall, The effect of ultrasound on water in the presence of dissolved gases, Can. J. Chem. 54 (1976) 1114–1120, https://doi.org/10.1139/v76-159.
[88] P. Supeno, Kruus, Sonochemical formation of nitrate and nitrite in water, Ultrason. Sonochem. 7 (2000) 109–113, https://doi.org/10.1016/S1350-4177(99)00043-7.
[89] C. Pe, C. Pulgarin, Bisphenol A Mineralization by Integrated Ultrasound-UV-Iron (II) Treatment, Environ. Sci. Tech. 41 (2007) 297–302, https://doi.org/10.1021/es061440e.
[90] M. Sivakumar, P.A. Tatake, A.B. Pandit, Kinetics of p -nitrophenol degradation : effect of reaction conditions and cavitational parameters for a multiple frequency system, Chem. Eng. J. 85 (2002) 327–338, https://doi.org/10.1016/S1385-8947(01)00179-6.
[91] Z. Guo, R. Feng, J. Li, Z. Zheng, Y. Zheng, Degradation of 2, 4-dinitrophenol by combining sonolysis and different additives, 158 (2008) 164–169. https://doi.org/10.1016/j.jhazmat.2008.01.056.
[92] P.R. Gogate, S. Mujumdar, J. Thampi, A.M. Wilhelm, A.B. Pandit, Destruction of phenol using sonochemical reactors: Scale up aspects and comparison of novel

configuration with conventional reactors, Sep. Purif. Technol. 34 (2004) 25–34, https://doi.org/10.1016/S1383-5866(03)00171-0.
[93] N.N. Mahamuni, A.B. Pandit, Effect of Additives on Ultrasonic Degradation of Phenol, Ultson. Sonochem. 13 (2006) 165–174, https://doi.org/10.1016/j.ultsonch.2005.01.004.
[94] J. Ueda, N. Saito, Y. Shimazu, T. Ozawa, A Comparison of Scavenging Abilities of Antioxidants against Hydroxyl Radicals, Arch. Biochem. Biophys. 333 (1996) 377–384, https://doi.org/10.1006/abbi.1996.0404.
[95] H. Sprinz, D. Beckert, O. Brede, Reactions of H atoms and OH radicals with ascorbic acid: a pulse radiolysis Fourier transform ESR study, J. Radioanal. Nucl. Chem. 232 (1998) 3–5, https://doi.org/10.1007/bf02383709.
[96] N. Mäkelä, T. Sontag-strohm, N.H. Maina, The oxidative degradation of barley B-glucan in the presence of ascorbic acid or hydrogen peroxide, Carbohydr. Polym. 123 (2015) 390–395, https://doi.org/10.1016/j.carbpol.2015.01.037.
[97] M. Curcio, F. Puoci, F. Iemma, O.I. Parisi, G. Cirillo, U.G. Spizzirri, N. Picci, Covalent insertion of antioxidant molecules on chitosan by a free radical grafting procedure, J. Agric. Food Chem. 57 (2009) 5933–5938, https://doi.org/10.1021/jf900778u.
[98] T. Wu, C. Wu, Y. Xiang, J. Huang, L. Luan, S. Chen, Y. Hu, Kinetics and mechanism of degradation of chitosan by combining sonolysis with H2O2/ascorbic acid, RSC Adv. 6 (2016) 76280–76287, https://doi.org/10.1039/c6ra11197a.
[99] Z. Zhang, X. Wang, X. Mo, H. Qi, Degradation and the antioxidant activity of polysaccharide from Enteromorpha linza, Carbohydr. Polym. 92 (2013) 2084–2087, https://doi.org/10.1016/j.carbpol.2012.11.096.
[100] S. Chen, H. Chen, R. Gao, L. Li, X. Yang, Y. Wu, X. Hu, Degradation of hyaluronic acid derived from tilapia eyeballs by a combinatorial method of microwave, hydrogen peroxide, and ascorbic acid, Polym. Degrad. Stab. 112 (2015) 117–121, https://doi.org/10.1016/j.polymdegradstab.2014.12.026.
[101] E.T. Urbansky, D.M. Freeman, F.J. Rubio, Ascorbic acid reduction of residual active chlorine in potable water prior to halocarboxylate determination, J. Environ. Monit. 2 (2000) 253–256, https://doi.org/10.1039/b001046o.
[102] E.T. Urbansky, K.M. Schenck, Ascorbic acid redaction of active chlorine prior to determining Ames mutagenicity of chlorinated natural organic matter (NOM), J. Environ. Monit. 2 (2000) 161–163, https://doi.org/10.1039/a909046k.
[103] S. Hassan, F. Adam, M.R.A. Bakar, S.K.A. Mudalip, Evaluation of solvents' effect on solubility, intermolecular interaction energies and habit of ascorbic acid crystals, J. Saudi Chem. Soc. 23 (2019) 239–248, https://doi.org/10.1016/j.jscs.2018.07.002.
[104] G. Kozmus, J. Zevnik, M. Ho, M. Petkov, Characterization of cavitation under ultrasonic horn tip – Proposition of an acoustic cavitation parameter, Ultrason. Sonochem. 89 (2022) 106159, https://doi.org/10.1016/j.ultsonch.2022.106159.
[105] G.E. Adjovu, H. Stephen, D. James, S. Ahmad, Measurement of total dissolved solids and total suspended solids in water systems: a review of the issues, conventional, and remote sensing techniques, Remote Sens. 15 (2023) 1–43, https://doi.org/10.3390/rs15143534.
[106] A.F. Rusydi, Correlation between conductivity and total dissolved solid in various type of water: a review, IOP Conf. Ser. Earth Environ. Sci. 118 (2018) 012019. https://doi.org/10.1088/1755-1315/118/1/012019.
[107] V. Distribution, The International Association for the Properties of Water and Steam, 2011.